

CHAPTER 2
LITERATURE REVIEW

CHAPTER 2

LITERATURE REVIEW

2.1 INTRODUCTION.

This chapter includes many previous researches which study the fire resistance of concrete and structural member's performance in a fire. Fire resistance is defined as the ability of the structure member to withstand exposure to a fire without loss of load bearing function or ability to act as a barrier to spread a fire.

2.2 Responses of Concrete to High Temperatures

2.2.1 Damage mechanisms of concrete under high temperatures

There are four types of major damage mechanisms responsible for deterioration of properties of concrete under high temperatures:

- (1) Phase transformations taking place in cement paste.
- (2) Phase transformations taking place in aggregate.
- (3) Thermal incompatibility between the cement paste and aggregate.
- (4) Spalling of concrete.

The first three damage mechanisms result in reduced strength and stiffness of concrete, while the last one leads to reduced cross section of structural members and loss of structural integrity.

2.2.1.1 Phase transformations in cement paste.

Major products of hydration reactions of Portland cement are Calcium Silicate Hydrates ($C_3S_2H_3$) or simplified as C-S-H, Calcium Hydroxide (CH), and Ettringite ($C_6AS_3H_{32}$). All of the hydration products decompose under high temperatures. The decomposition processes of the hydration products at various temperature ranges are listed in **Table 2.1** [Schneider 2002].

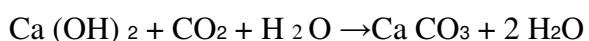
Temperature range [°C]	Transformation or decomposition reaction	Heat of reaction or transformation [kJ/kg]	Heat of reaction or transformation [MJ/m ³ concrete]	Mass of reaction [kg/m ³ concrete]
30 - 120	Desorption or evaporation of physically adsorbed water	Heat of evaporation of water: 2258	290	130 kg water
30 - 300	gel destruction: 1. stage of dehydration	Heat of hydration: 250	< 20	< 78 kg hardened cement paste
120 - 600	Release of chemically adsorbed or zeolithically bonded water	Heat of evaporation of water: > 2258	> 135	60 kg water
450 - 550	Decomposition of portlandite $\text{Ca}(\text{OH})_2 \rightarrow \text{CaO} + \text{H}_2\text{O}$	1000	< 40	< 40 kg CaO
570	Transformation of quartz $\alpha \rightarrow \beta \text{SiO}_2$	5,9	8,8 1,2	1500 kg quartz 200 kg quartz
600 - 700	Decomposition of CSH-phases; formation of $\beta\text{-C}_2\text{S}$	Heat of hydration: 500	< 120	< 240 kg hardened cement paste
600 - 900	only calcite: dissociation of calcite	Heat of decomposition: 1637	2360	1600 kg limestone CaCO ₃ -content approx. 90 %
from 1100 - 1200	Melting of concrete, formation of glassy materials	Melting heat: 500 - 1000	quartzitic: 1575 calcitic: 1125	2100 kg concrete 1500 kg concrete

Table 2.1:Decomposition of cement paste at various temperatures ranges [Schneider 2002].

The chemical reactions for the decomposition processes can be described as following:



The formation of CaCO₃ is due to accelerated carbonation reaction of CH,



Then, CaCO_3 decomposes at high temperatures. Water evaporates under high temperatures. Associated with the formation of new phases in the chemical reactions are changes in volume as well as in stiffness of cement paste. There are cracks and voids formed in cement paste along with the decomposition of CH, which results in major damage of concrete. Similarly, the stiffness of the new products is different from the stiffness of the original phases, which leads to a change in stiffness of concrete when temperature rises.

2.2.1.2 Phase transformations in aggregates.

For normal weight concrete, there are two common aggregate groups: siliceous aggregates such as quartzite, gravel, granite and flint; calcareous aggregates such as limestone, dolomite and anorthosite. It is generally known that siliceous aggregates, especially quartzite, experience phase transformation at approximately $T = 570^\circ\text{C}$ from α -quartz to β -quartz. This crystal transformation is reversible and endothermic which involves a heat of transformation of 5.9kJ/kg of SiO_2 . Assuming about 75 percent of the quartzitic aggregate in the concrete participates in the transformation, the heat of transformation is found to be 8.8 MJ/m^3 for quartzitic and about 1.2 MJ/m^3 for calcitic concrete.

2.2.1.3 Thermal incompatibility between cement paste and aggregate.

Concrete is a composite material with aggregates as inclusions and cement paste as matrix. The two phases have different thermal and mechanical properties and thus respond differently upon a temperature rise. The aggregates in concrete expand with increasing temperature. Cement paste may expand if the thermal expansion is dominant and may shrink if the moisture loss is dominant.

The combined effect of the deformation mechanisms of the two phases depends on many factors such as heating rate, holding period, and composition of the concrete. **Fig 2.1** illustrates these effects. The thermal incompatibility between the two phases causes very large mismatch in the deformation between aggregates and cement paste, which results in cracks in the interfacial transition zone around aggregates. Subsequent heating, drying, and loading may cause coalescence of the cracks to form discrete large cracks leading to spalling of concrete and/or failure of concrete structures.

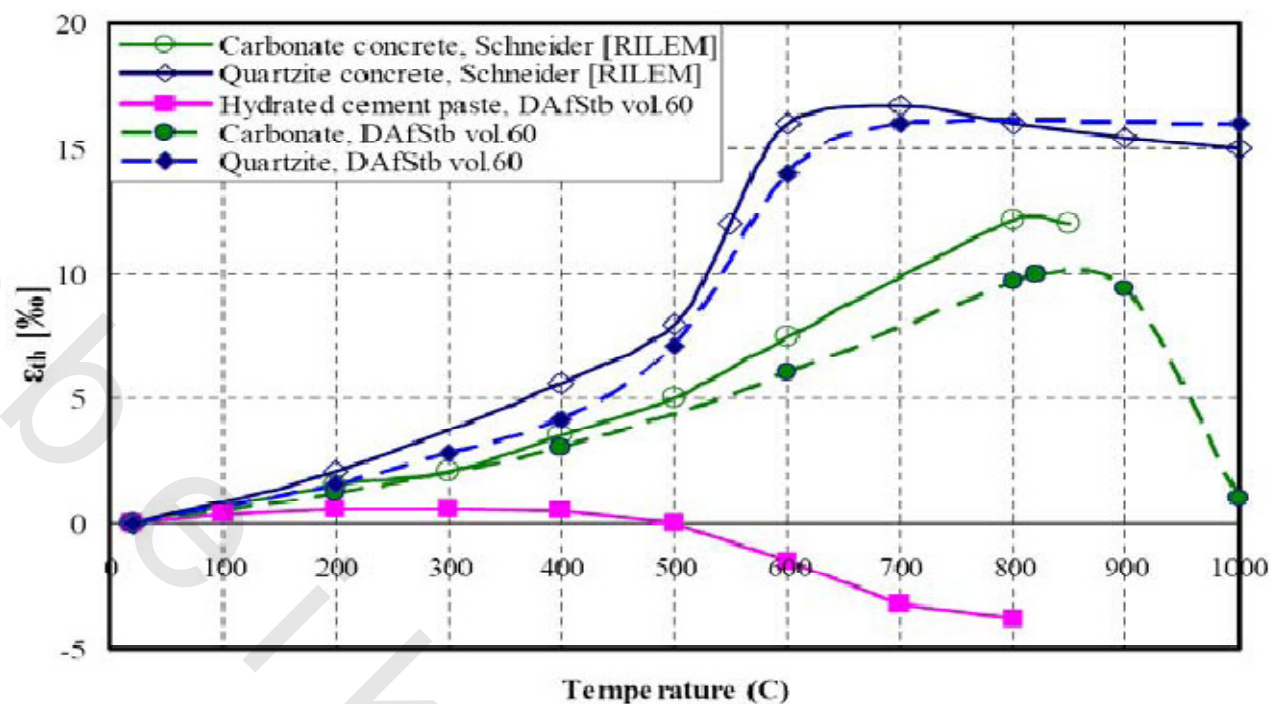


Fig. 2.1 Thermal strains for different concretes, aggregates and hydrated cement paste.

2.3 Actual State of the Codes on Fire Design in the Different Countries.

Many codes and countries produce standards for design and improve resistance the concrete to fire.

2.3.1 Actual State of the Codes on Fire Design in Japan.

In this paper, the state-of-the-art of fire resistance design of concrete in Japan is summarized into two parts. First part corresponds with structure of building regulations on fire resistance of buildings. The second part is associated technical standards for reinforced concrete and composite structures of steel and concrete.

2.3.1.1 Summary of performance-based changes in Building Standards Law of Japan

The building code of Japan (Building Standards Law of Japan, BSLJ, hereafter) was revised in 2000, including performance-based sentences for fire resistance. A simplified performance evaluation method was provided for various types of structures including concrete.

A- Requirements

The BSLJ was revised in 1998 to include functional requirements in place of detailed technical specifications of materials and constructions. Even though it is not perfect, the law has

shifted towards performance-based format. Following the changes in law, enforcement order (detailed items of regulation) and notifications (technical standards) were revised in June 2000. Concerning with the structural fire resistance, performance evaluation framework and a set of simplified calculation formula have been added as Kensho (verification method) for fire resistance. By using verification method, it is possible to check the adequacy of fire resistance of structural elements easily and quickly.

B-Functional approach

After the revision, it is possible to adopt functional approach in fire resistance design. The objective implied in BSLJ is to prevent;

- (1) Collapse due to fires that are foreseeable to take place in the building,
- (2) Fire spread to the buildings during fires that normally takes place around the building.

The functional requirements to satisfy the objective are;

- (1) Load-bearing structural part shall sustain load throughout the complete process of fire.
- (2) Building envelope (exterior walls and roofs) shall not create a gap that may penetrate flame from inside to outside
- (3) Floors and internal firewalls shall not create a gap to penetrate flame nor transmit heat enough to ignite combustibles in the opposite side of fire compartment in both directions.
- (4) Exterior walls shall not transmit heat enough to ignite combustibles in the building.

The above requirements are summarized in **Fig.2.2**.

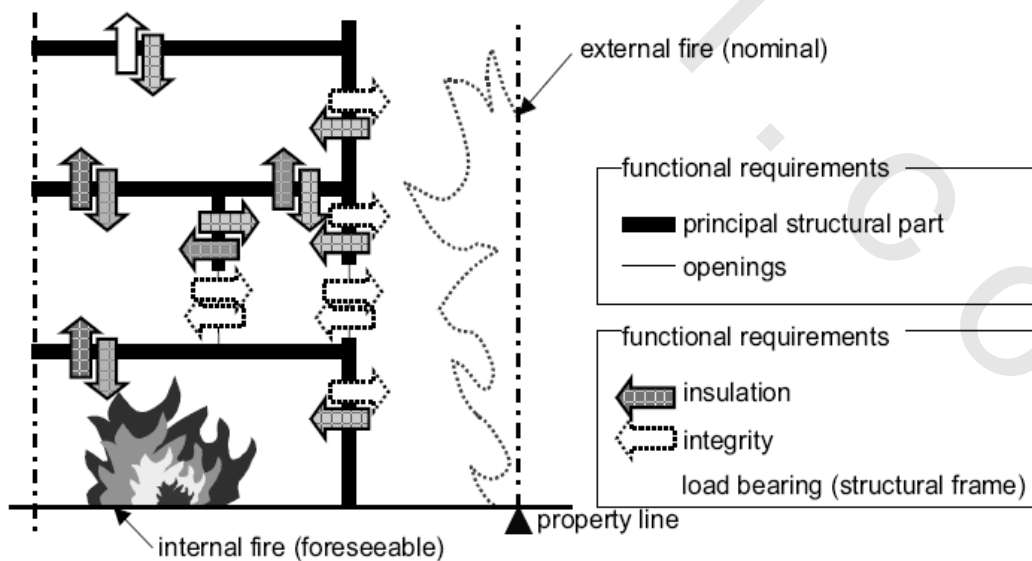


Fig. 2.2-Functional requirements for fire resistance.

C- Performance evaluation

To satisfy the requirement of BSLJ, planning body can choose among Route A, B and C. As shown in **Fig. 2.3** route A is a conventional method that follows prescriptions in the code. Code specifies required fire resistance time of principal structural part depending on size (number of stories) of buildings. The principal part shall be made of fire resistive constructions listed in approved constructions. As to concrete-frame buildings, minimum dimensions (diameter and cover thickness) are prescribed as shown in **Table 2.2**. Performance-based routes were provided as in route B and C. Route B is to apply simplified design formula specified in MoC's notification 1433(2000fy). The chance is at most increased if they choose Route C. The difference between route B and C are the degree of sophistication and complicity of design process, and the body that will review design solution. In the Route B, design process is simplified enough so that local building authority can review the design solution themselves. In practice, it means that review and approval process is finished quickly, but at the same time, the design would have to be conservative. In route C submittals, it is possible to adopt any design procedure as long as it follows the requirements of law and as long as it is correct in engineering sense. The appropriateness is judged by a peer-review body, followed an approval by MLIT (Minister of Land, Infrastructure and Transportation).

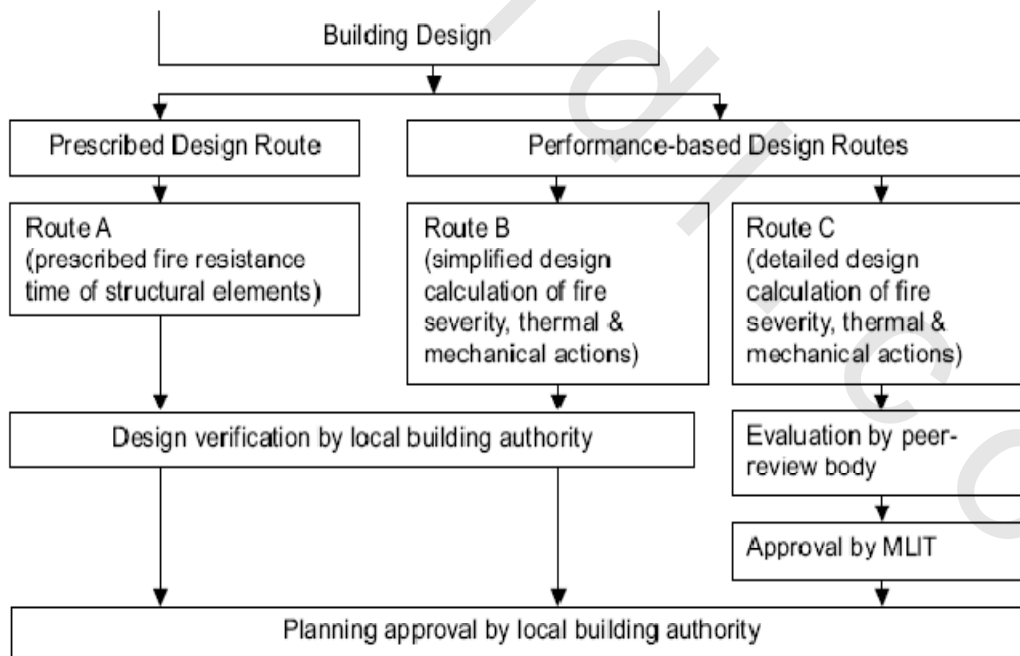


Fig. 2.3- Three Routes to Conform with Fire Resistance Requirements in BSLJ.

Table 2.2 Deemed-to-satisfy Specifications inBSLJ.

element of construction	fire resistance rating [min]	minimum dimension [mm]	minimum cover thickness [mm]
wall, floor	60	70	(not specified)*
column	120	100	30
	60	(not specified)	30
	120	250	50
beam	180	400	60
	60	(not specified)	(not specified)*
	120	(not specified)	50
	180	(not specified)	60

* Minimum value are specified in terms of durability (20mm for floors, 30mm for columns and beams)

2.3.1.2 Design methods.

Depending on the type of concrete, design methods are selected as follows for most cases.

A- Reinforced concrete of ordinary strength.

For ordinary strength concrete (design strength $F_c > 60\text{N/mm}^2$), simplified design method can be applied.

1- General principle.

The general principle for structural fire resistance is to prevent the strength reduction of loadbearing elements. Namely the strength (resistance) R must be larger than the service load S throughout the fire process,

$$R(t) > S(t), t = 0 \sim \infty \text{ ----- Eq.(1)}$$

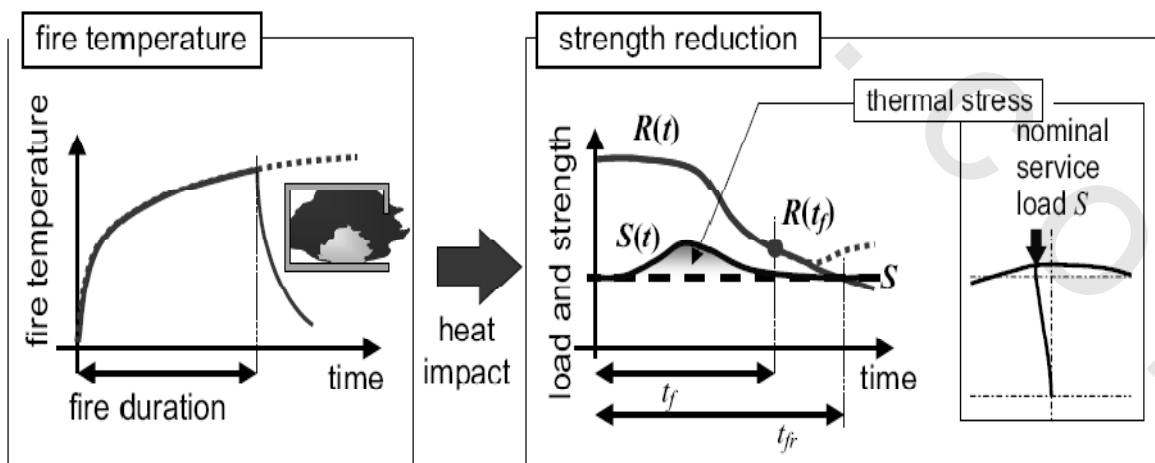


Fig.2.4 - Typical changes in load and strength of steel column during fire.

The typical changes in strength and service load are shown in **Fig.2.4**. Service load increases due to the thermal stress in the early stage of fire. However, at the critical condition of structural endpoint, thermal stress is negligible. This assumption is valid for ductile structures designed against wind and earthquake motion. As a result of seismic resistance design, structural frame is equipped with enough deformation capacity so that the frame is insensitive to perturbations caused by thermal stress in the early stage of fire.

Following above assumption, it is practical to check the strength at the fire duration (plus some post fire period) $t = t_f$. Equation (1) could be

$$M = t_f(S) - t_f > 0,$$

Where S is the load applied by external force. It is more convenient to express by time margin, $t_f(S)$ is the critical time to failure under the service load S .

Calculation procedure consists of two parts. The first half is to calculate the fire severity of all the potential fire rooms. The second half is to calculate the time to failure of structural element.

2- Calculation of time to structural failure.

Fig 2.5 shows the calculation procedure for time to structural end point. The procedure starts with calculation of structural forces during normal condition to determine minimum cross sectional area for load bearing. Then the time to critical thermal deterioration depth (ineffective section, usually taken by 500°C isothermal line) is calculated.

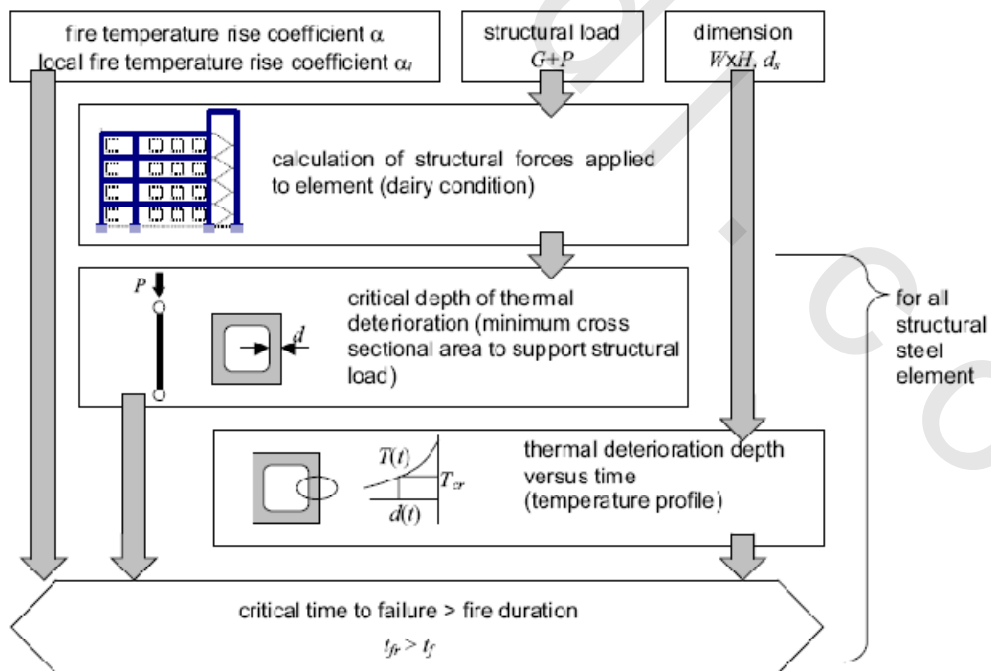


Fig. 2.5 - Calculation Procedure of Critical Time to Failure by Simplified Verification Method.

a) Design strength at high temperature

Fig. 2.6 shows existing results of compressive strength of concrete at high temperature. For most cases, strength is reduced gradually in the temperature range of 300 and 800°C. At 500°C, strength decreases to about 2/3 of nominal design strength at normal temperature. To make conservative estimate of strength at high temperature, it is assumed that

$$F_c(T) = \begin{cases} (2/3)F_c(20) & (20 \leq T \leq 500) \\ 0 & (500 < T) \end{cases}$$

where $F_c(20)$ is nominal design compressive strength at normal temperature.

b) Temperature profiles

For a concrete members heated by ISO834 standard fires

$$T_f - T_0 = 345 \log_{10}(8t + 1) \approx 460t^{1/6}$$

The temperature profile can be approximated by

$$\frac{T(x, t) - T_0}{460t^{1/6}} = \exp\left(-\frac{cx}{\sqrt{t}}\right)$$

Where c is a coefficient depending on the type of material ($c=0.21$ for normal weight concrete, 0.23 for lightweight concrete). After mathematical approximations, the final form is

$$T(x, t) = 713(cx)^{1/3} \exp\left(-1.4 \frac{cx}{\sqrt{t}}\right) + T_0,$$

Which is graphically shown in Fig. 2.7.

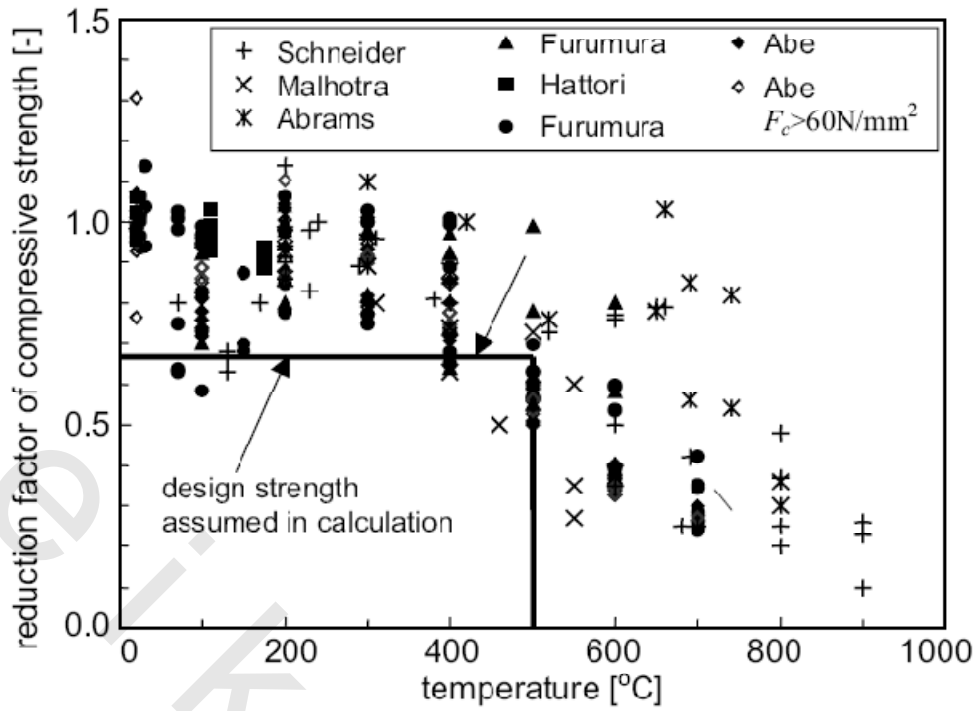


Fig. 2.6 Compressive strength of concrete at high temperatures and design strength (Abrams, 1971).

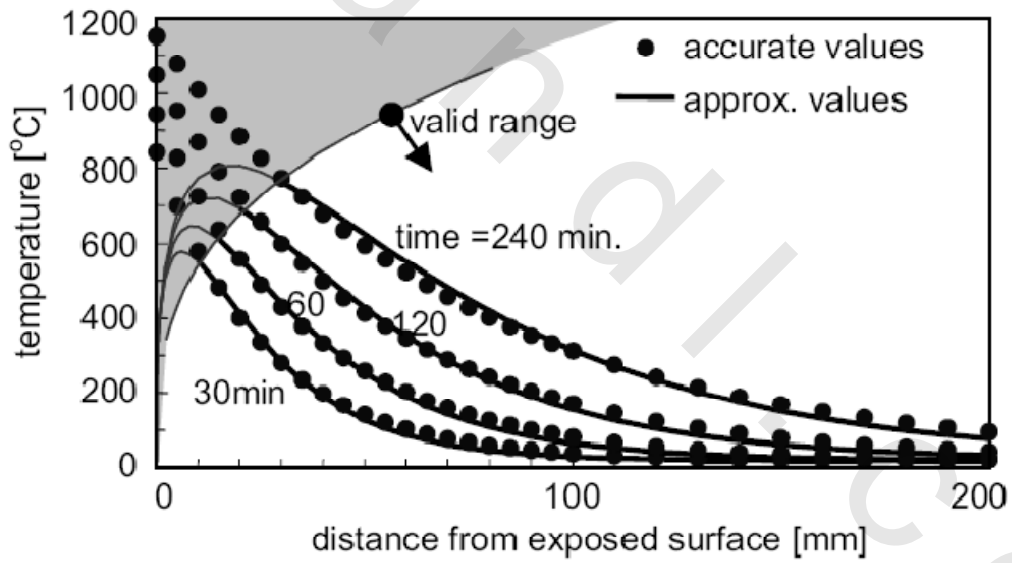


Fig. 2.7 - Temperature profiles against distance from fire-exposed surface as a function of Time.

2.3.2 Actual State of the Codes on Fire Design in Europe.

2.3.2.1 Status and background.

European standard EN 1992-1-2 Eurocode 2: Design of concrete structures – Part 1.2: General rules – Structural fire design was approved in Formal Vote in June 2004 and it is expected to be published by the end of 2004. European countries have to implement it as national standard. Some safety related numerical values may be chosen or modified in National Annex which should be published in two years. Present national standards may coexist until year 2010. EN 1992-1-2 is a revised version of European prestandard ENV 1992-1-2, published in 1995 for experimental use.

Fire design rules in Eurocode 2 are based on CEB Bulletins on Fire Design of Concrete Structures, latest edition N° 208 July 1991. Adaptation to the Eurocode system has been done, tabulated data on columns has been completely revised, high strength concrete has been added and some other modifications have been made.

EN 1992-1-2 is intended to be used in conjunction with

- EN 1990 Basis of structural design
- EN 1991-series Actions on structures
- EN 1992-1-1 Design of concrete structures – General rules and rules for buildings background documentation is available on DIN Livelihood for European Standard Bodies

2.3.2.2 Fire actions and load level.

Actions in fire situation are taken from EN 1991-1-2 Actions on structures exposed to fire. Mechanical actions are reduced by combination factors which depend on the type of load. Recommended partial factors for actions and materials are = 1.0. As a simplification the effects of actions may be obtained from a structural analysis for normal temperature design as:

$$E_{d,fi} = \eta_{fi} E_d$$

Where:

E_d is the design value of the corresponding force or moment for normal temperature design, for a fundamental combination of actions,

η_{fi} is the reduction factor for the design load level for the fire situation.

Reduction factor η_{fi} is explained in **Fig. 2.8**. A safe side estimation $\eta_{fi} = 0.7$ may be used.

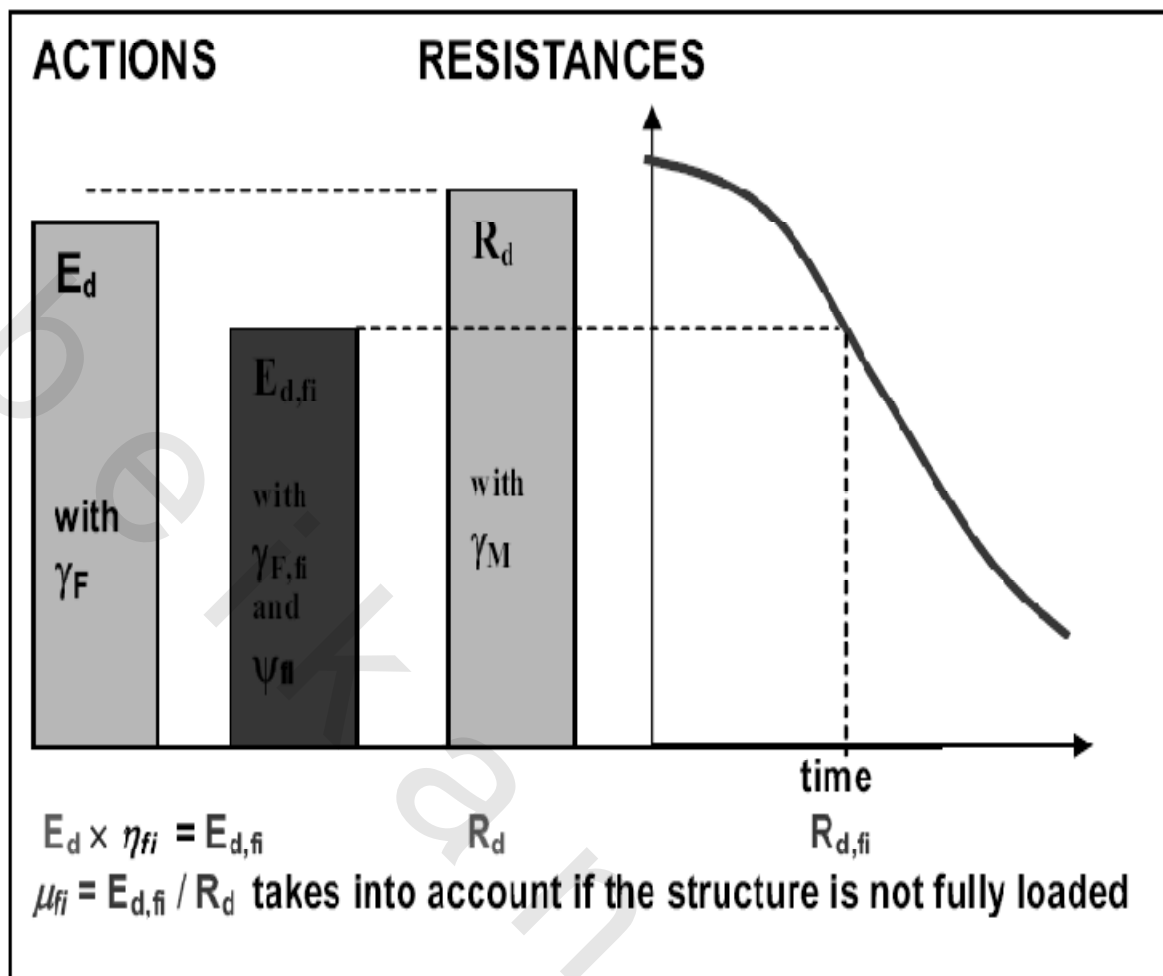


Fig. 2.8- Load level in fire design.

2.3.2.3 Design methods.

In principle there are three assessment methods: tabulated data, simplified calculation methods and advanced calculation methods. For advanced calculation methods the principles only are given. Two optional simplified calculation methods are included: 500°C isotherm method as in CEB N° 208 and zone method as in ENV 1992-1-2. In the first one concrete with temperature above 500°C is disregarded and full strength is used for the rest of cross-section. In the second one the cross section is divided into zones and more accurate strength value in each zone is used in calculations. Design methods are illustrated in Fig. 2.9.

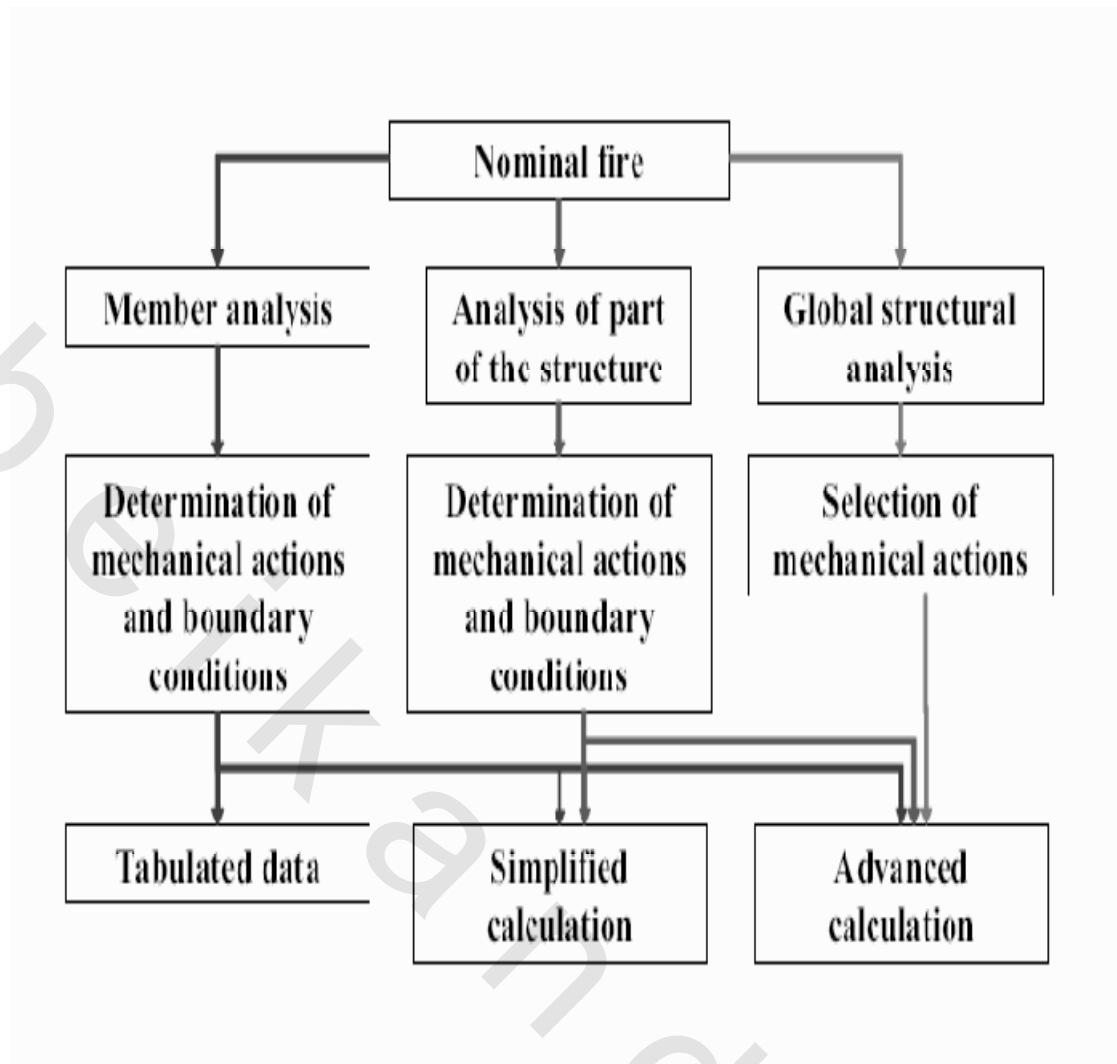


Fig. 2.9- Design methods for standard fire.

2.3.2.4 High strength concrete.

Rules for high strength concrete have been included. Strength reduction at elevated temperatures depends on the composition and constituents of concrete. National Annex may choose strength reduction from three recommended classes, see **Fig. 2.10**. There are four optional methods against spalling, surface reinforcement mesh, tested type of concrete, protective layers or polypropylene fibers.

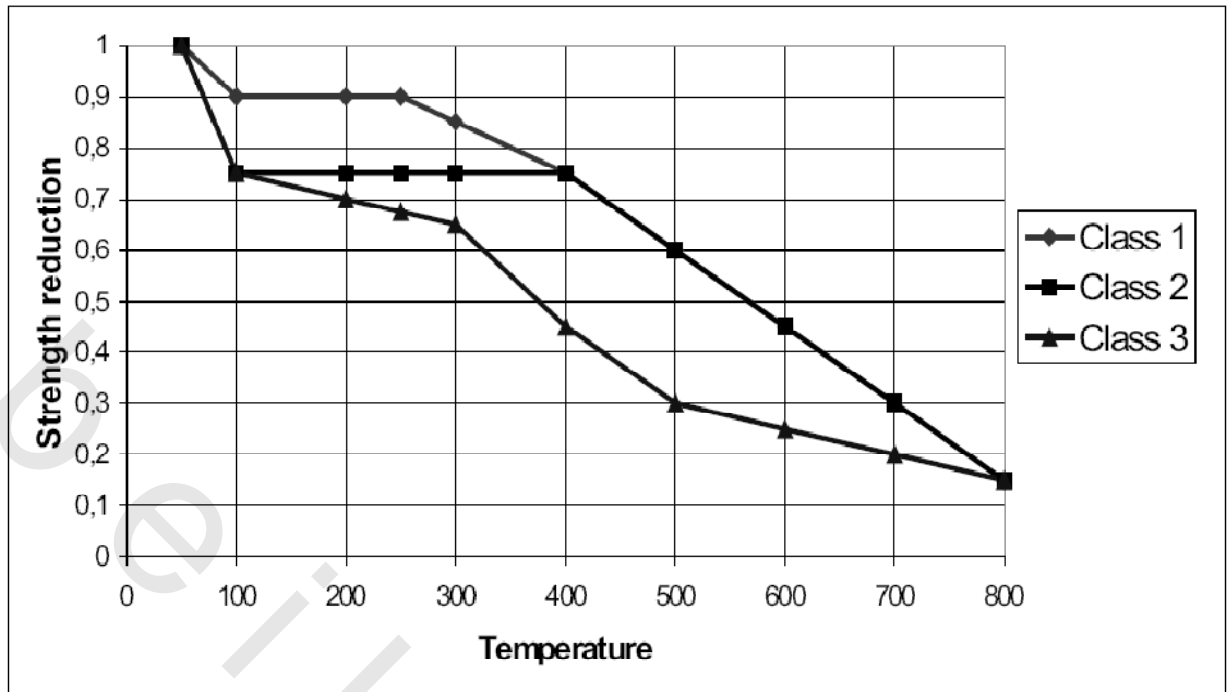


Fig. 2.10 - High strength concrete, strength reduction classes.

2.3.2.5 Shear, torsion and anchorages.

Simplified calculation rules for shear, torsion and anchorage are given in an informative annex. These rules give guidance how to define the reference temperature of shear reinforcement. It is reminded that non-linear temperature distributions may cause tensile stresses, reducing shear capacity for some types of cross sections. The reference temperature p should be evaluated at points P along the line 'a-a' for the calculation of the shear resistance. The effective tension area A may be obtained from EN 1992-1(SLS of cracking), see Fig. 2.11.

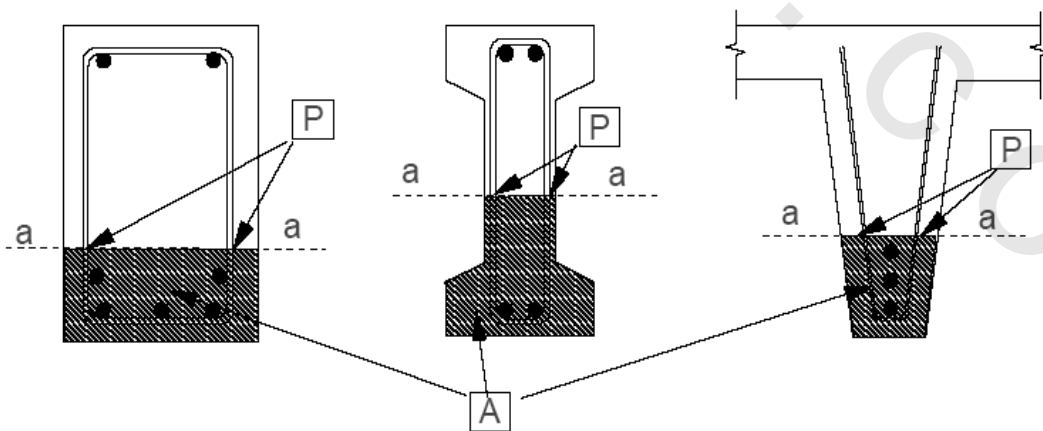


Fig. 2.11- Reference temperature for shear reinforcement.

2.3.3 Summary of current US Codes and Standards and their applicability.

Provisions for fire protection of structures prescribed by the model codes are adopted, in whole or in part, by the building codes of different states or local jurisdictions in the U.S. These fire protection provisions are handled separately from the structural design procedures for other loads such as snow, wind, gravity, and earthquake loads. The sections below summarize the scope of the fire protection provisions of the two current US model codes and the relevant standards that are referenced by these codes.

A-IBC 2000

The objectives of **IBC 2000's** fire protection provisions are primarily to ensure life safety (of building occupants and emergency fire responders) and, to a lesser extent, to provide a measure of property protection. These objectives can be achieved by using fire-resistance-rated constructions with fire resistance ratings that meet the prescribed minimum requirements and by complying with other requirements for active fire protection measures. IBC 2000 prescribes the following methods for determining fire resistance ratings of different building components or subassemblies:

- Qualification testing: based on standard fire exposure and test procedure set forth in **[ASTM E119 Standard Test Methods for Fire Tests of Building Construction and Materials]**.
- Fire resistance designs documented in approved sources.
- Prescriptive designs of fire-resistance-rated building elements: based on tabulated data provided by the code for different structural parts
- Calculated fire resistance method: for concrete, the prescribed methods for calculated fire resistance ratings of different assemblies are those prescribed by **[ACI/TMS 216 Standard Method for Determining Fire Resistance of Concrete and Masonry Assemblies]**.

In addition to these methods for determining fire resistance ratings of structural components, IBC 2000 also specifies prescriptive requirements for other fire protection measures such as the types and locations of fire protection systems (automatic sprinkler systems, standpipe systems, fire alarm and protection systems, smoke control systems, smoke and heat vents, etc...) and the means of egress. A brief description of ASTM E 119 and ACI/TMS 216, which are referenced by IBC 2000, is given below.

1- ASTM E 119.

ASTM E 119 specifies laboratory procedure and criteria for determining fire resistance ratings of building components or assemblies exposed to a prescribed standard time-temperature history. This standard time-temperature history does not represent real fire conditions, which can vary with compartment size and configuration, ventilation, and fuel loads. The results of this standard test are meant to provide a relative measure of the fire test response, in terms of fire resistance ratings, of comparative test components and assemblies, and are not meant to provide an assessment the structural performance of the tested elements. Fire testing of concrete components and assemblies in accordance with ASTM E 119 is often controlled by the following two acceptance criteria:

- Heat Transmission Criterion: which requires sufficient thickness of concrete is provided to limit unexposed surface temperature rise of walls, floors, and roofs.
- Load Carrying Ability Criterion: which requires sufficient thickness of concrete cover is provided so that the yield strength of steel reinforcement is at least 50% of that at ambient temperature.

2- ACI/TMS 216.

Standard ACI/TMS 216 is referenced by IBC 2000 as an approved method for calculating fire resistance ratings of concrete, concrete masonry, clay brick and tile masonry assemblies. This standard does not apply to composite metal deck floor or roof assemblies. Except for continuous concrete slabs and beams, where ACI/TMS 216 provides procedures for calculating fire resistance ratings, guidance for concrete columns and walls are strictly based on prescriptive tabulated data.

The fire resistance rating calculated or determined by methods prescribed by ACI/TMS 216 is also based on the standard fire exposure prescribed in [ASTM E 119]. The current version of ACI/TMS 216 does not specify a range of concrete compressive strengths for which its provisions and calculation methods are applicable. In the calculation methods prescribed for concrete slabs and beams, ACI/TMS 216 allows the concrete compressive strength, f'_c , to vary as a function of temperature. However, this compressive strength-temperature relationship is mainly based on one set of experimental data obtained for normal strength concrete [Abrams M.S., 1971] and thus might not be applicable when concrete with higher strength grade is concerned.

a) ACI specifications on the strength of concrete under high temperatures

The current ACI code, ACI/TMS-216 was developed based primarily on the early test data by Abrams (1971), which showed the temperature dependence of the uniaxial concrete compressive strength as shown in Fig. 2.12, 2.13, and 2.14 are taken from ACI/TMS-216 on “Fire Resistance” of concretes with three different types of aggregates. The figures illustrate the reduction of compressive strength of $f_c = 3900$ psi concrete in the temperature range up to $T = 1600^\circ\text{F}$. The general trends show that axial pre-loading $\sigma_{pre} = 0.4 f_c$ leads to higher strength properties when compared to unstressed conditions. Furthermore, residual strength after cooling leads to far greater degradation of strength than hot testing.

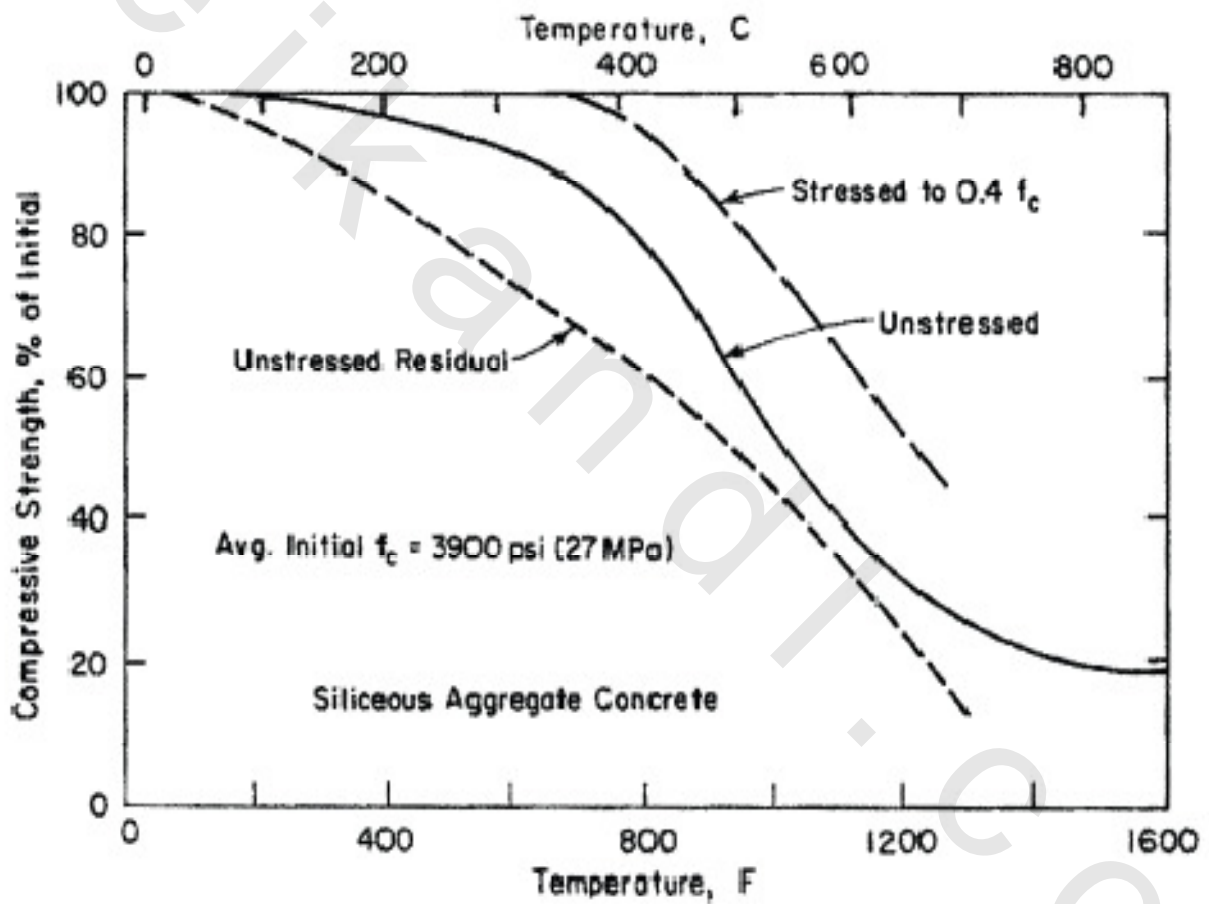


Fig. 2.12-Compressive strength of siliceous aggregate concrete: [ACI-216].

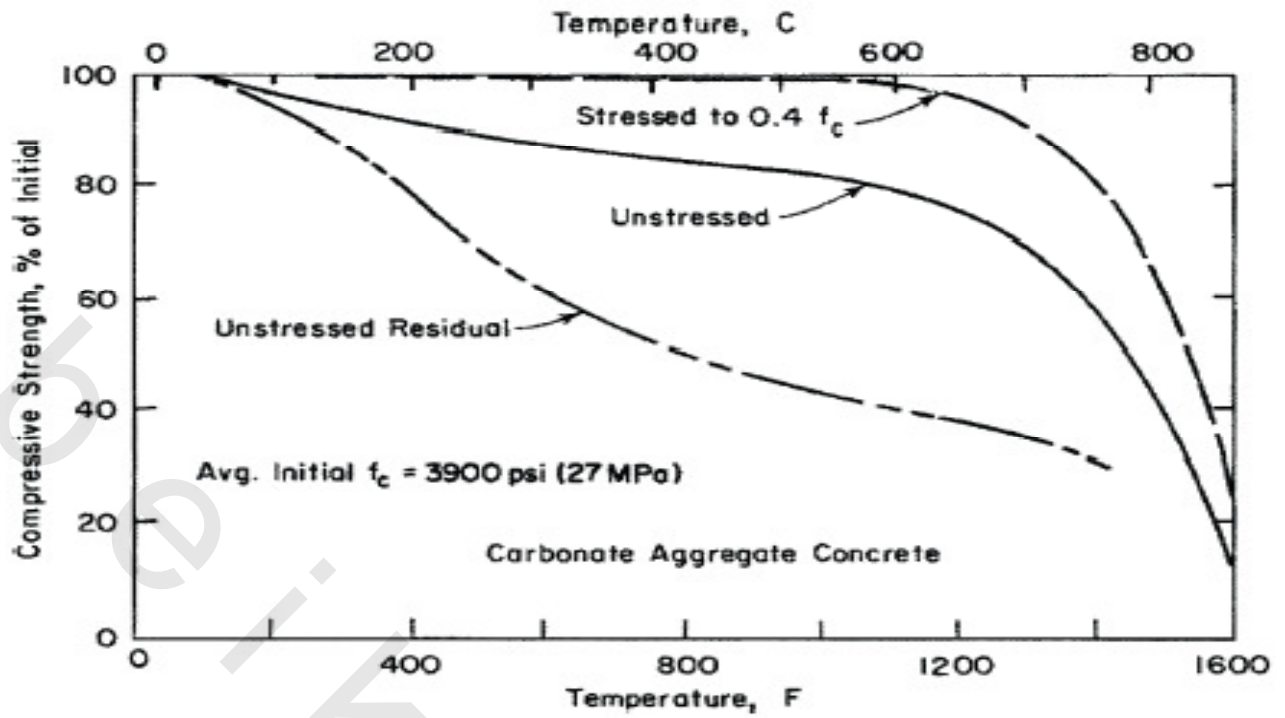


Fig. 2.13-Compressive strength of carbonate aggregate concrete: [ACI-216].

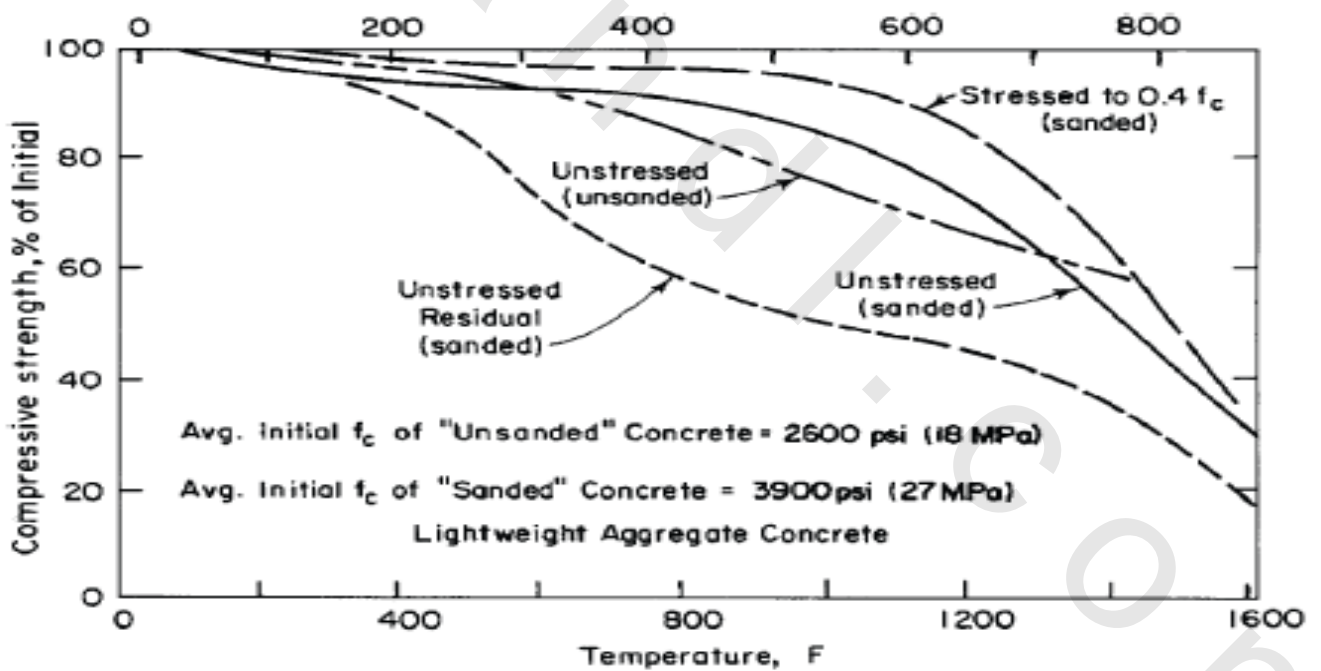


Fig. 2.14-Compressive strength of semi-lightweight concrete: [ACI 216].

From Figs. 2.12, 2.13, and 2.14 it is clear that ACI-216 provisions do not call for degradation of the temperature dependent strength properties when prestressing and hot test

conditions (stressed to 0.4 f_c') are considered for all three types of aggregates. Whereas the hot strength of siliceous concrete as seen in **Fig. 2.12** does not decrease up to 200°F = 93°C, the residual strength (unstressed residual cold testing) exhibits less than 5% degradation below the reference unloaded concrete compression strength. Interestingly enough, both hot and residual carbonate aggregate concrete as shown in **Fig. 2.13** exhibit higher degradation properties than siliceous aggregate concrete up to 200°F = 93°C. However the reduction relative to the reference unloaded concrete compressive strength is still less than about 5%. The main difference between siliceous and carbonate aggregate concrete appears at higher temperatures. For the semi-lightweight concrete, the degradation of the concrete under hot test conditions started at about 100°C, but the degradation is not significant up to 500°C. It should be pointed out that caution must be used in the practice, because the properties of lightweight concrete really depend on the type of lightweight aggregate used in the concrete.

B- NFPA 5000.

In terms of fire protection, the objectives of model code NFPA 5000 are similar to IBC 2000's. NFPA 5000 provides prescriptive requirements for fire protection of fire walls, fire barrier walls, horizontal assemblies, exterior walls, smoke barrier, vertical openings, mezzanine, joints, concealed spaces, etc. and specifies the following methods for determining fire resistance ratings of fire resistive materials and constructions:

- Qualification testing: based on standard fire exposure and test procedure set forth in **NFPA 251 Standard Methods of Tests of Fire Endurance of Building Construction and Materials.**
- Analytical methods: as prescribed by **ASCE/SFPE 29 Standard Calculation Methods for Structural Fire Protection for Structural Elements or Assemblies** or **ACI/TMS 216 Standard Methods for Determining Fire Resistance of Concrete and Masonry Assemblies.**
- Other approved analytical methods based on the fire exposure and acceptance criteria specified in NFPA 251.

A brief summary of ASCE/SFPE 29 and NFPA 251 is provided below. ACI/TMS 216 is also referenced by model code NFPA 5000 and its summary has been provided in the above section.

1- ASCE/SFPE 29.

ASCE/SFPE 29 provides calculation methods for determining equivalent fire resistance ratings for selected structural members and barrier assemblies made of steel, concrete, concrete masonry, clay masonry, and wood that would have been achieved in the ASTM E 119 standard fire test. Thus, as is the case for ACI/TMS 216 standard, the fire resistance ratings calculated using this standard do not necessarily describe performance for natural fires having a time-temperature relationship different from that prescribed by ASTM E 119. The concrete provisions of ASCE/SFPE 29 are applicable to: (1) plain, reinforced, and prestressed concrete made with cementitious materials, aggregates (siliceous, carbonate, sand-lightweight, lightweight); (2) concrete with specified compressive strength f'_c not exceeding 69 MPa; (3) cast-in-place, precast, and slabs cast on stay-in-place steel forms where slab is designed to carry all superimposed loads including the slab deadload; (4) walls – single and multi-wythe; (5) floors – single and multi-layer, restrained and unrestrained; (6) roofs – with and without insulation, restrained and unrestrained; (7) beams – restrained and unrestrained; and (8) columns.

Except for the method for calculating the fire resistance ratings and concrete cover for flexural members (provided by ACI/TMS 216 and not provided by ASCE/SFPE 29) and the range of applicable concrete compressive strength (limited to 69 MPa in ASCE/SFPE 29 and not defined in ACI/TMS 216), the calculation methods for concrete components prescribed by ASCE/SFPE 29 are mostly identical to those prescribed by ACI/TMS 216.

2- NFPA 251.

NFPA 251 Standard Methods of Tests of Fire Endurance of Building Construction and Materials prescribes laboratory procedures and methods for qualification testing of building materials and assemblies subjected to a standard time-temperature history. The standard time-temperature history and most of the test procedure and requirements specified by NFPA 251 are identical to those specified by ASTM E 119. One minor difference between these two standards is that NFPA requires the furnace temperatures to be recorded at intervals not exceeding 1 min during the test period, while ASTM E 119 requires the furnace temperature to be recorded at intervals not exceeding 5 min during the first 2 h of the test, and thereafter at intervals not exceeding 10 min.

2.4 PERFORMANCE-BASED STRUCTURAL FIRE ENGINEERING (PBSFE).

While the field of Performance-Based Structural Fire Engineering is in the developmental stage, the overall structure of the process has been well defined for some time.

[Grosshandler,2002]outlined the process in summarizing a recent fire resistance workshop. The processincludes both design and analysis components. The analysis components involve the definitionof the design fire exposure, the thermal/mechanical response of the structural assembly(including any fireproofing materials), and structural response of the structural system. Thebroader design processes are shown in **Fig.2.15**, including inputs from building coderequirements and inputs from assembly listings. Here we take a broad view of assembly listingsto include any engineering data that can be deduced from the testing involved in the developmentof the listing (despite the fact that such test data is not made public by the listing organization ortest sponsors at the current time) or fire resistance testing not associated directly with the listingprocess. The recommendations developed in this report are intended to provide additionalengineering information and data from the activity noted in **Fig. 2.15** as “Assembly Listing andData.” These infrastructure components are shown above the dashed line, while the actualdesign portion of the process is shown below the dashed line. The design components includethe architectural and structural designs of the building, which form the basis for the fireengineering design.The fire engineering begins with the development of a design fire exposure to the structure.This normally takes the form of a time-temperature curve based upon the fire load, ventilation,and thermal properties of the bounding surfaces (walls, floor, and ceiling). Design fire loads aredependent upon the occupancy and other fire protection features of the building. Significantly,with respect to furnace testing, the performance of the boundaries to limit fire spread is theprimary component of defining the design fire area. Often the exposed fire area is defined byboundaries with sufficient fire resistance to prevent fire spread under the design fire load density.It is significant to note that the time-temperature curves developed in compartment fires mostoften exceed the time-temperature curves used in the test methods like **[ASTM E 119]**. As notedby **[Drysdale ,1999]**, this has been recognized but tacitly accepted since the 1920s in the settingof prescriptive fire resistance requirements for buildings.Based upon the architectural and structural designs, the design fire is used to develop thepassive fire protection design. This involves the selection of fire resistive assemblyconstructions for use as walls, columns, and floor/ceiling assemblies. The assemblies areselected to survive the design fire exposure, to be consistent with the architectural/structuraldesign, and to provide cost-effective protection. It would be normal to develop more than oneset of conceptual designs for further evaluation.

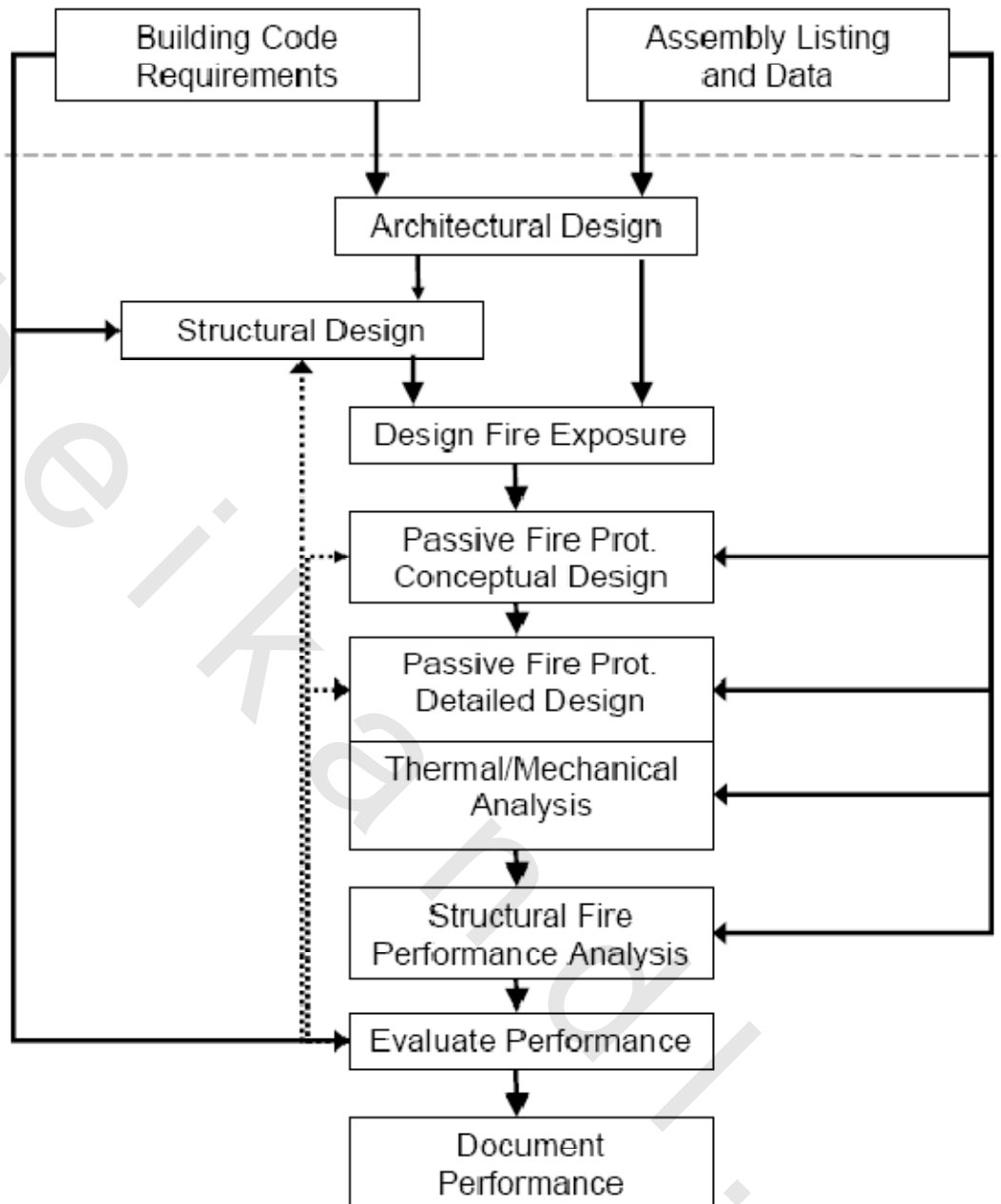


Fig. 2.15-Performance-based structural fire engineering (PBSFE) design process.

Detailed design involves the use of thermal/mechanical models to assess the performance of each conceptual design, resulting in trial protection thicknesses based upon tentative thermal failure criteria. It is typical to perform two-dimensional heat-transfer analyses, but three-dimensional analyses are sometimes required. It is significant that existing models cannot deal with the mechanical performance of the assembly in any substantive manner. Loss of physical integrity of a material or the assembly cannot be modeled at this time. The designer relies entirely upon the results of testing to assure that physical integrity is maintained over the design exposure

period. In most cases, the engineer will seek to use materials and assemblies that can be relied upon to maintain integrity, or alternatively simple, and somewhat ad hoc, assumptions about material loss are made in the design calculations. The final analysis process is the prediction of structural performance of the structure under design loads with the structural elements heated according to the heat-transfer analysis. This analysis can be performed for individual elements, for the substructure in the fire area, or for the complete structural system. Typically, multiple analyses are performed with more detailed analysis at the element level and more basic analysis at the structural system level. Based upon the performance of the system, redesign may be indicated. This could include changes to the structural design (especially if changes here could allow removal of fireproofing altogether), changes in the passive design concept (e.g., change insulating material), or alterations in the detailed design of the passive fire protection (modify the thicknesses of the insulation). Other redesign aspects are possible, but these are the most common.

As indicated the assembly listing and data that is, or could be, included in the listing documentation can contribute to the passive fire protection design, the thermal/mechanical analysis, and the structural fire performance analysis. It is important to note that the listing documentation (e.g., the test report) is not a public document under the current system so that these can only be used with the assistance of the owner of the listing. In addition, the current listing may not be directly supported by reported tests. Testing may have been performed with an old version of the protective material and the current material may be accepted under the listing based upon the listing agency's engineering judgment. While this may be satisfactory for prescriptive use of the product, it has serious limitations with respect to PBSFE. Other data sources, not shown in **Fig. 2.15**, also contribute to these design and analysis processes. These include other published data concerning temperature dependent structural properties of materials and thermal properties of insulating materials. While some of this data is produced using standard methods, other data is obtained via ad hoc testing methods. The analysis methods employed in the design process may vary from special purpose software to general heat-transfer or structural analysis software. Some software is developed by the designer, some is developed by government laboratories, and some is commercial software. There is a specific need to address applicability, validation, and verification of these methods for use in specific Performance-Based Structural Fire Engineering (PBSFE) designs. It is the vision of this report that a fire resistance test in support of PBSFE should be a part of the validation and verification (V&V) basis for the application of analysis tools to specific fire resistance designs. All needed data to support the analysis should be developed through tests designed for that purpose

(e.g., thermal properties and structural properties). The furnace test should be conducted and instrumented to provide high quality data and boundary conditions to form a data set that can be predicted using the analysis tools. The successful prediction of the test would form a partial basis for demonstrating the applicability of the models to the particular fire resistance design. The test would further identify any mechanical behaviors such as erosion, cracking, spalling, shrinkage, fastener failures, warpage, and other behaviors that need to be mitigated in the design or accommodated in the design calculations. There is a wide range of testing and reporting aspects of standard fire test methods that are required to support PBSFE. These include simple characterization of the test article and the properties of the component materials, as well as substantive measurements made and the conduct of the test itself. It has been recognized for many decades that realistic fire exposures can exceed the exposure in ASTM E 119 and that the exposure conditions to the assembly vary among furnaces operated in a manner consistent with existing test methods. There is also a need to develop and validate thermal properties of insulating materials and the methods and instrumentation of standard test methods to support PBSFE. There are definite unresolved issues concerning the structural conduct of the test to assure that the results are applicable to long spans and connections found in actual construction. This brings to the fore issues of structural scaling laws, and the use of structural rather than thermal endpoints for the test. Issues also exist with the conduct of the test with respect to failure criteria. Valuable failure mode data can be provided by the practice of “testing to failure.” These and other issues have received varying levels of attention in the testing and research literature. There is no doubt that a new fire resistance test method can become a valuable tool in PBSFE design. The recommendations included in the following sections are in support of this objective.

2.5 Compressive strength of concrete under high temperatures.

The compressive strength of concrete at high temperature is largely affected by the following factors:

- 1) Individual constituent of concrete.
- 2) Sealing and moisture conditions.
- 3) Loading level during heating period.
- 4) Testing under ‘hot’ or ‘cold residual’ conditions.
- 5) Rate of heating or cooling.
- 6) Duration under an elevated temperature (holding period).

7) Time maintained in moist conditions after cooling before the strength test is carried out.

8) Number of thermal cycles [Khoury, 2002]. Before discussing thermal responses of concrete under high temperatures, it is important to distinguish several different loading scenarios for strength testing. Three testing methods are commonly used to examine the strength and stiffness of concrete under a high temperature. These testing methods are referred to as stressed tests, unstressed tests, and unstressed residual strength tests [Phan, 1996]. The schematic of the three test methods is shown in Fig. 2.16.

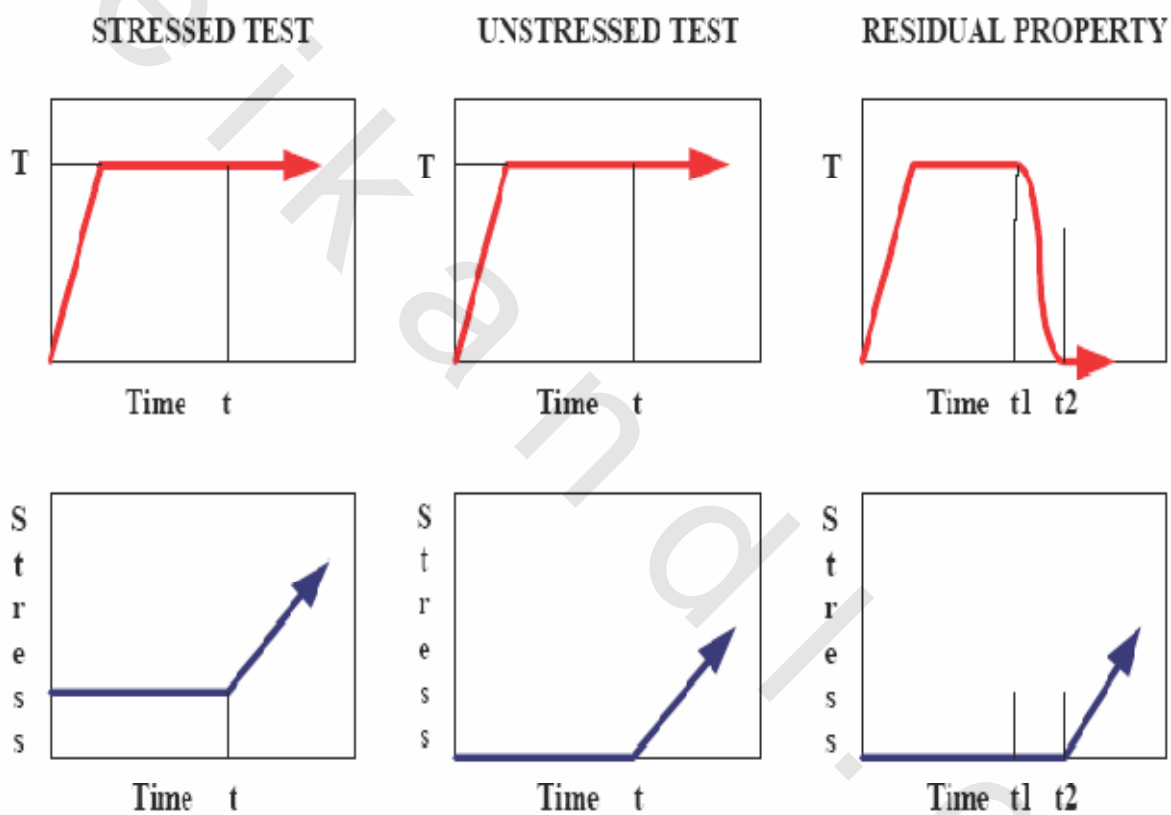


Fig. 2.16-Schematic of temperature and loading histories for the three test methods.

Stressed test is a test in which a preload, generally in the range of 20 percent to 40 percent of the ultimate compression strength of concrete at room temperature, is applied to the concrete specimen prior to heating, and the load is sustained during the heating period. After the specimen reaches a steady state temperature condition, the stress or the strain is increased to a prescribed loading rate until the specimen fails. The test results of this test are most suitable for representing fire performance of concrete in a column or in the compression zone of beams and

slabs where the structural member is suddenly subjected to an overload during fire due to failure of other structural member.

Unstressed test is similar to the stressed test except that the preload level is zero. The concrete is unstressed prior to the final loading. The test results are most suitable for representing the performance of concrete elements with low stress levels under service conditions and loaded under high temperatures.

Unstressed residual strength test is a test in which the specimen is cooled to room temperature after one or several cycles of heating without preloading. The mechanical load is then applied (after the heat treatment) at room temperature under stress or strain control until the specimen fails. The results of this test are most suitable for assessing the post fire (or residual) properties of concrete.

All three test methods can be used to determine the compressive strength (the maximum stress), the modulus of elasticity, the strain at the maximum stress, and the dissipated mechanical energy as a function of temperatures.

It has been established that compressive strength of concrete decreases with increasing temperature. However, determination of the temperature at which the reduction of strength should start is not an easy task. This is mainly because test data do not show the simple monotonic decreasing trend for concrete strength as shown in ACI 216, instead, many test data showed that the strength of concrete decreases first, and regains or even exceeds the original strength in the temperature range of 100 to 200 °C, and then decreases with further temperature increase. This phenomenon may be described as a first down, then up, and further down trend (or simply the down-up-down trend) in compressive strength of concrete under high temperatures. There are some explanations on the physical mechanisms responsible for the down-up-down trend, although there is no widely accepted theory validated by systematic experimental studies. The current design codes did not consider such a variation in strength of concrete under high temperature.

[Bažant, Z., et al. 1979] as illustrated in Figs 2.17 and 2.18 summarizes early test data from different researchers. They show large scatter of hot and cold (residual test) experiments which resulted from a number of different mix designs and testing conditions. One can see from the figures that some of the curves showed the variation of compressive strength in the low temperature range (the down-up-down trend). One should keep in mind that the tests were performed under unsealed and unstressed conditions, whereas testing of sealed specimens

would further reduce the strength values because of internal pore pressures generated by high temperatures.

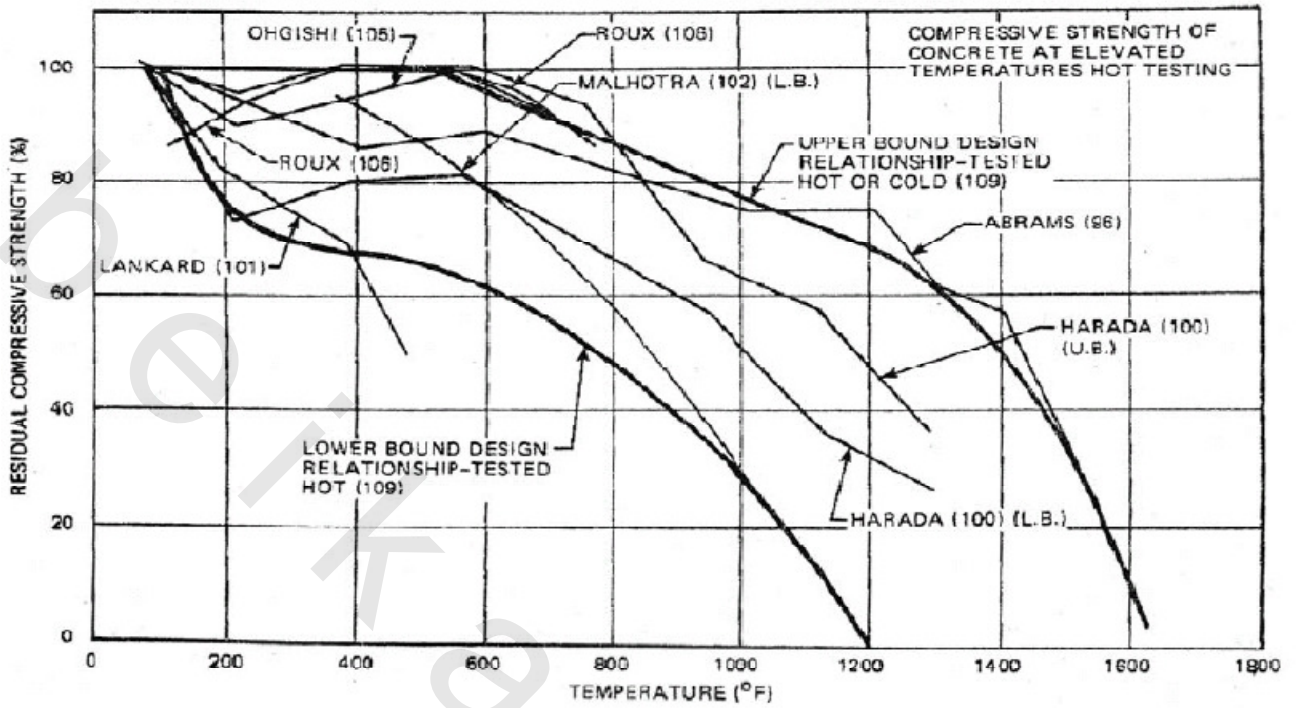


Fig. 2.17-Temperature sensitivity of compressive strength when tested at elevated temperature [Bažant, Z., et al. 1979].

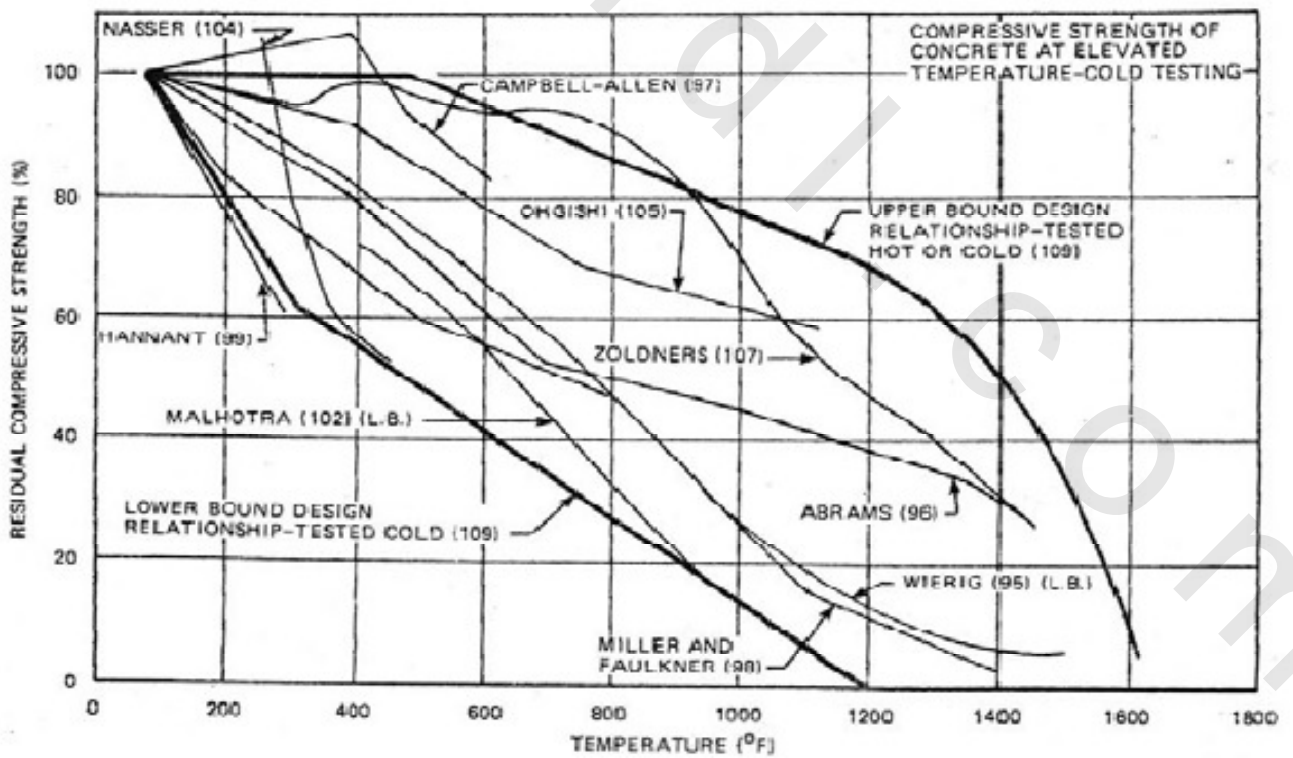


Fig. 2.18-Temperature sensitivity of compressive strength when tested cold (unsealed-unstressed), [Bažant,Z.,et al. 1979].

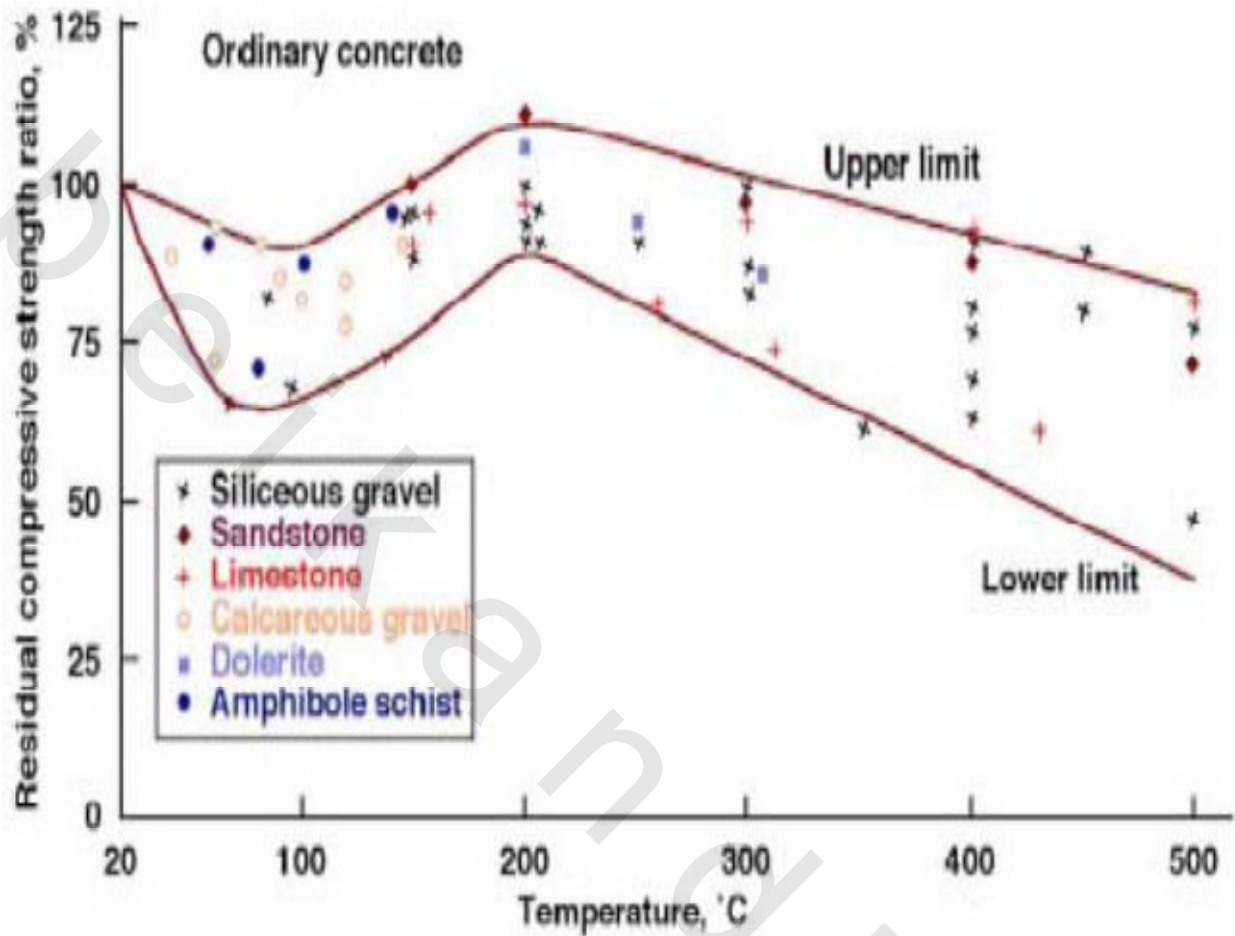


Fig. 2.19- Effect of aggregate on concrete strength materials exposed to high temperatures, Blundell et al (1976).

[Blundell, Diamond and Browne, 1976] published the early test data see Fig. 2.19, which illustrates more clearly the down-up-down trend of concrete strength in the range of $T = 50 \sim 200^{\circ}\text{C}$. The compression strength of concrete drops, regains and even exceeds at 200°C thereference strength at room temperature depending on the aggregate and moisture condition. Whereas these variations depend strongly on the aggregate type, they disappear at temperature exposures above 200°C when the strength decreases progressively as expected in oven-dry concrete materials.

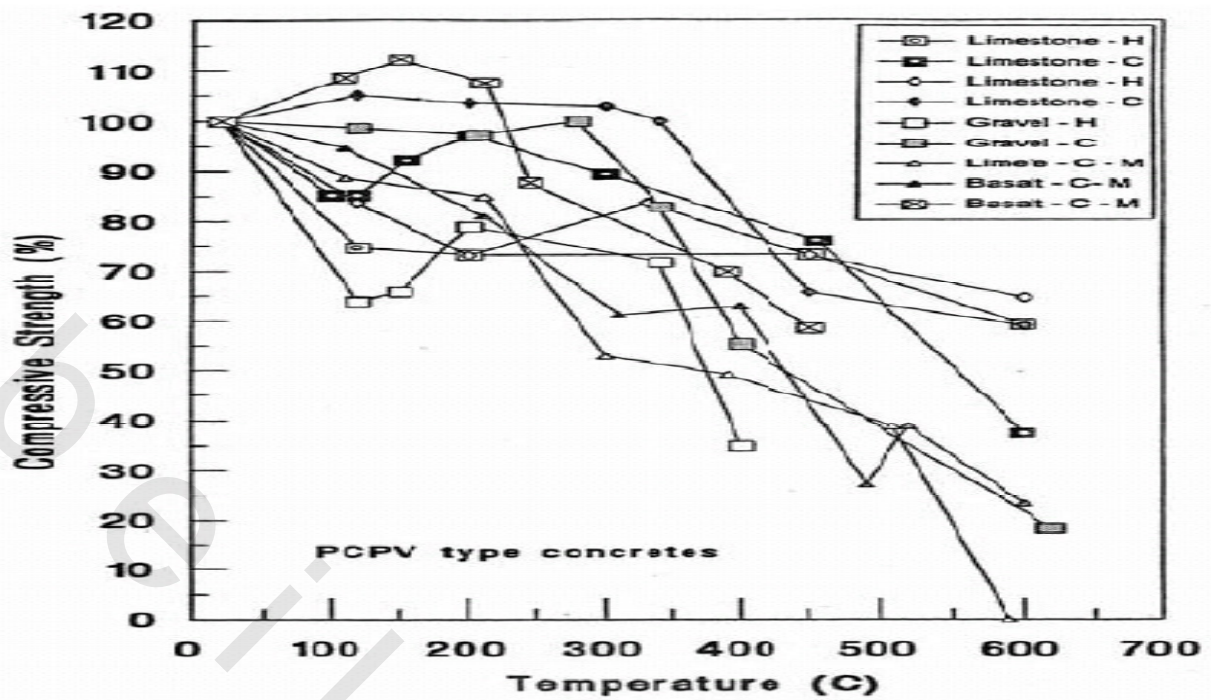


Fig. 2.20-Unsealed PCPV concrete specimens tested hot (H) and cold (C), Khoury (1984).

Similar observations to the early test data [Blundell, Diamond and Browne 1976] were made by [Khoury, 1984] which are reproduced in Fig. 2.20. The data demonstrate the strong influence of aggregate type on the temperature sensitivity of strength of pressure vessel concrete when tested hot (H) and cold (C).

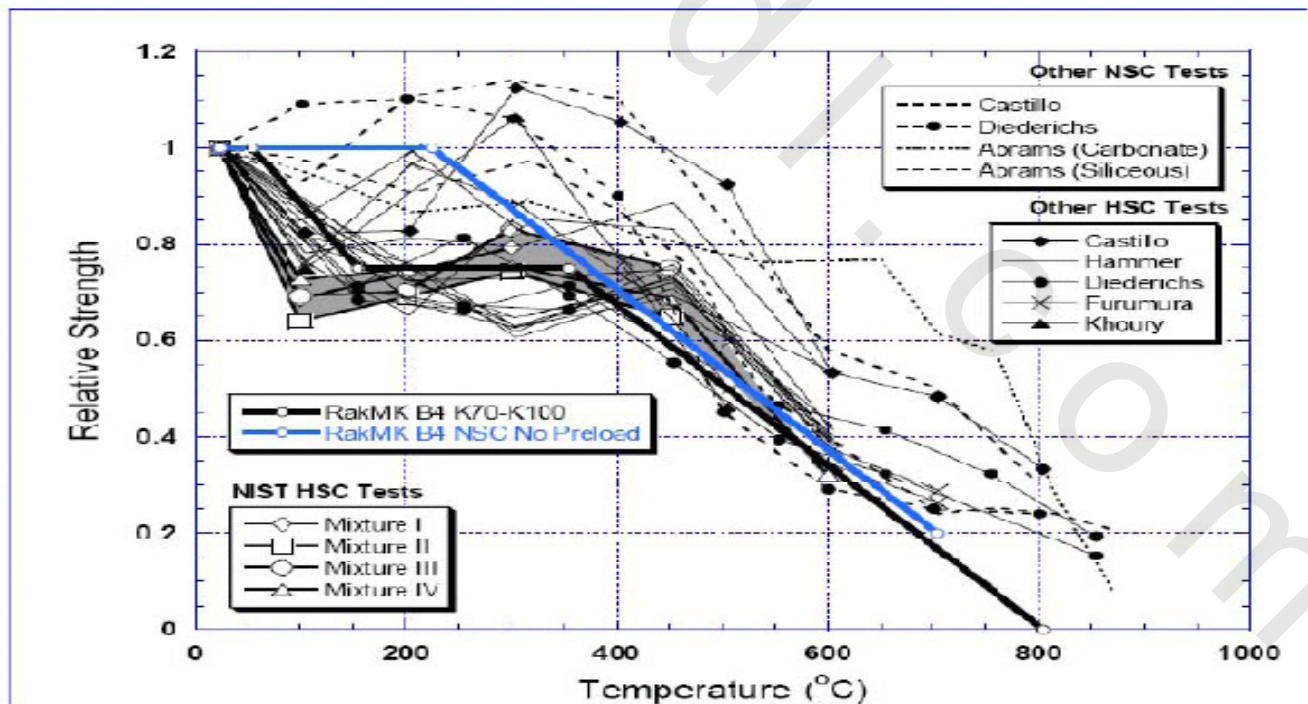


Fig. 2.21-Unstressed High Temperature Data of NSC vs HSC, Phan and Carino (2003).

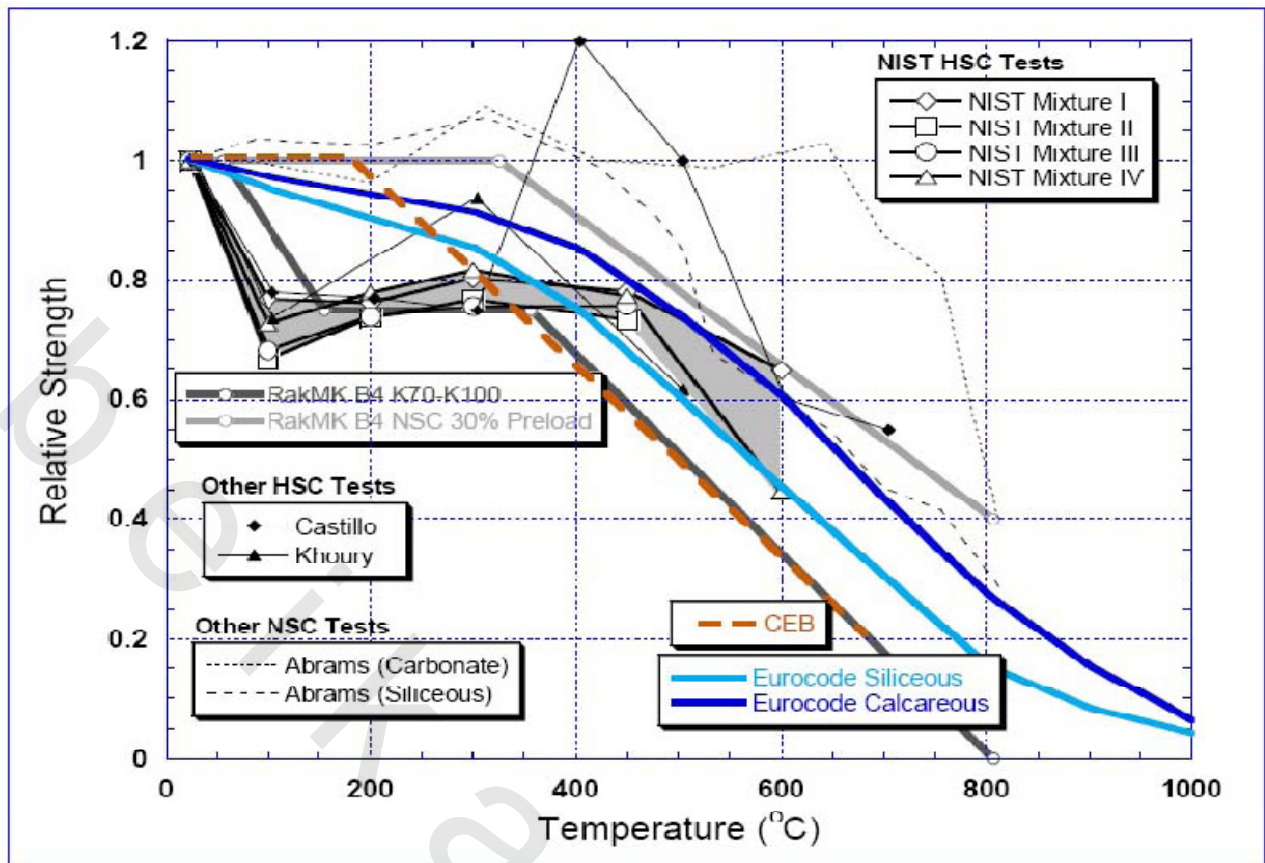


Fig. 2.22-Stressed High Temperature Data of NSC vs HSC, Phan and Carino (2003).

Evaluating temperature effects on HPC, [Phan and Carino, 1998] presented NIST data of a broad experimental program using hot testing with and without preloading. They compared the test results of different HPC mix designs with related design rules. Figs. 2.21 and 2.22 compare NSC and HSC test data with the predictions of the Finnish Design Code RakMK B4 which was at that time the only fire code separating temperature limits for HSC and NSC. Whereas there is no degradation of the compressive strength beyond 200°C in the case of normal strength concrete, both Figs. 2.21 and 2.22 illustrate the early reduction of compressive strength of the high strength concrete data at 100°C down to 72% of the reference strength at room temperature. On code specifications for the starting temperature for strength reduction, ACI 216 was based on [Abrams, 1971] test data, and the strength reduction started from very low temperature ranging depending on loading conditions and aggregate types, as shown in Figs. 2.12, 2.13, and 2.14. Reviewing the provisions for temperature dependent strength values in ASCE Manual No 78 (1992) and Eurocode EN 1992-1-2 (2004) we note that the temperature dependent compressive strength is not reduced for temperatures $T \leq 100^\circ\text{C}$, i.e. $f_c^T / f_c' = 1$. In contrast to normal strength concrete this temperature reduction factor diminishes to $f_c^T / f_c' = 0.75$ for high

strength concrete which was discussed by [Phan and Carino, 1998], and was further examined very recently by [Kodur et al. 2008] in the context of fire resistance of high strength concrete. A very recent study of high temperature compression data was presented by [Kodur et al. 2008]. Figs 2.23 and 2.24 compare test data on NSC and HSC tested under hot conditions with the predictions of Eurocode EC2 for siliceous and carbonate concretes. Whereas there is no degradation of the compressive strength up to 200°F in the case of normal strength concrete, Fig. 2.24 illustrates the early reduction of compressive strength down to 75% when high strength concrete is tested at 200°F.

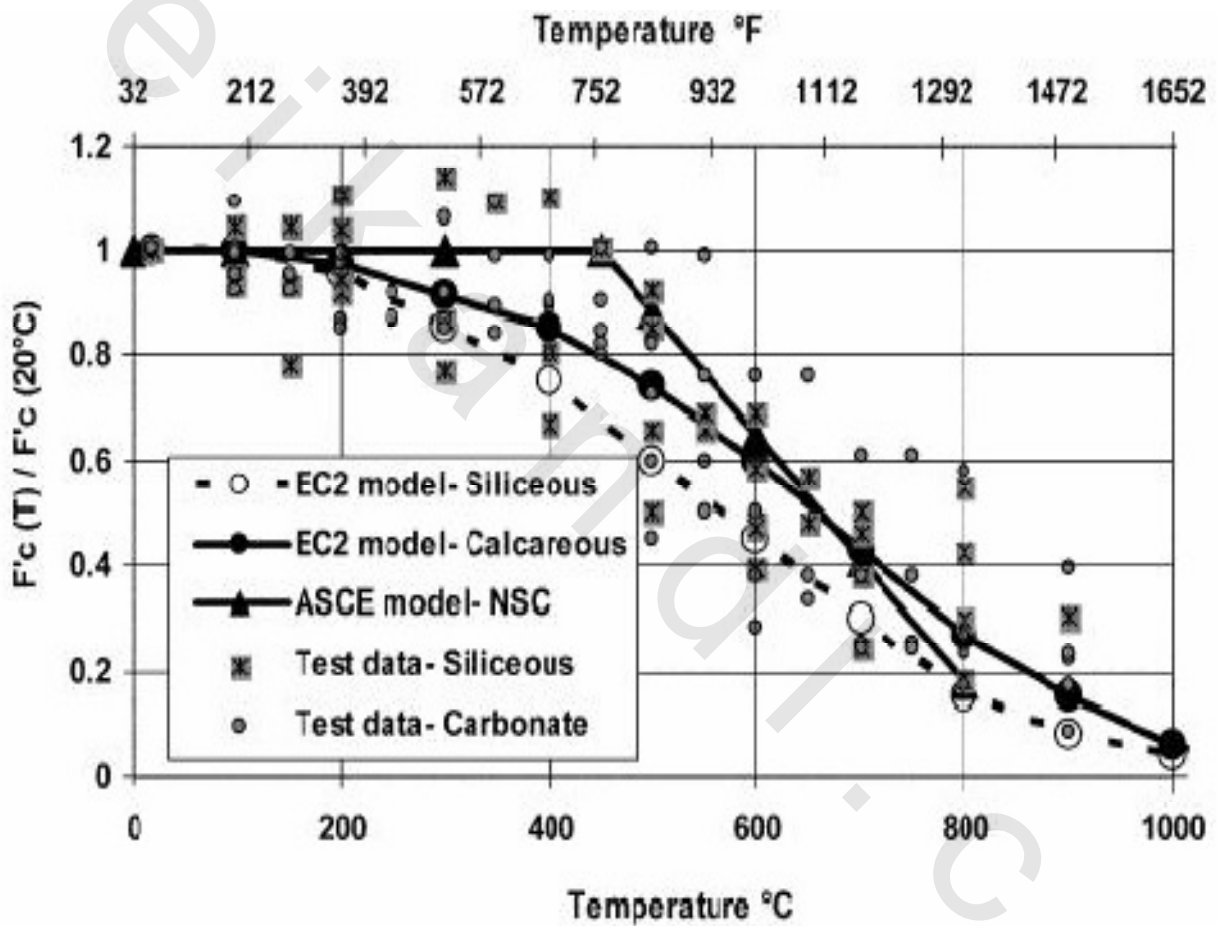


Fig. 2.23 High Temperature Models for NSC Concrete, Kodur et al. (2008).

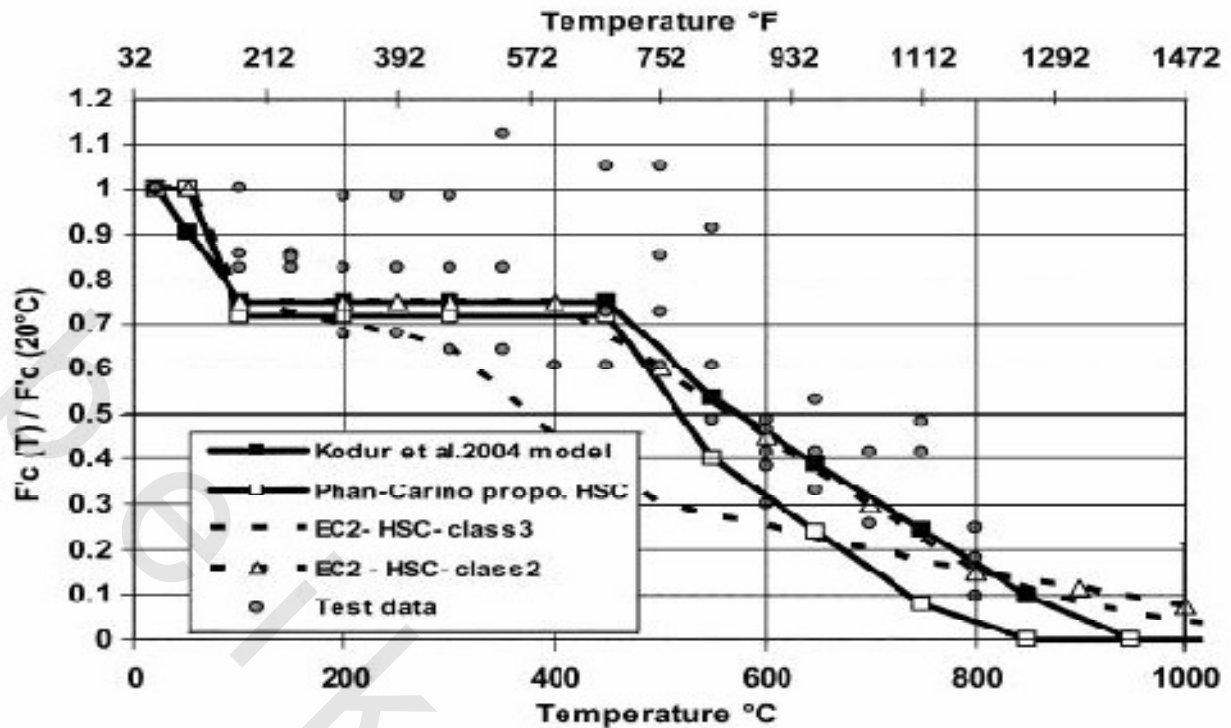
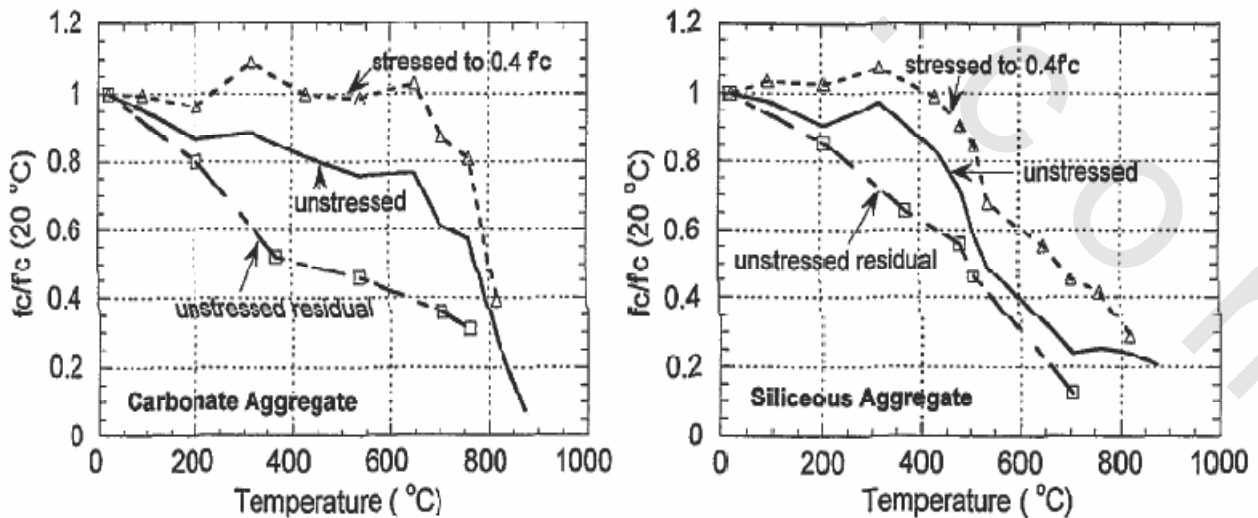


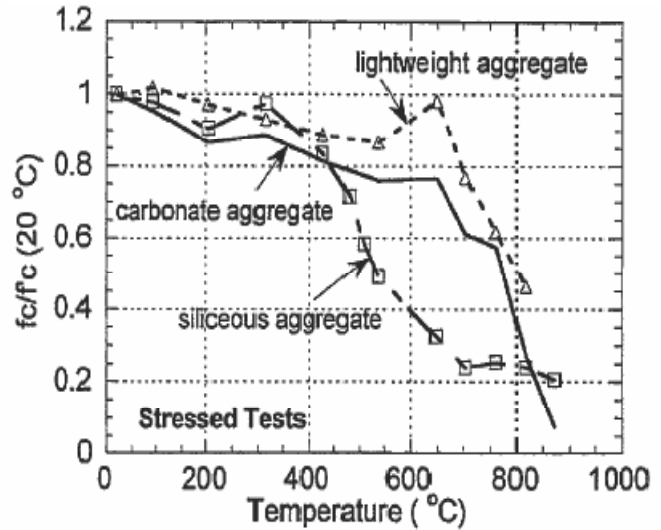
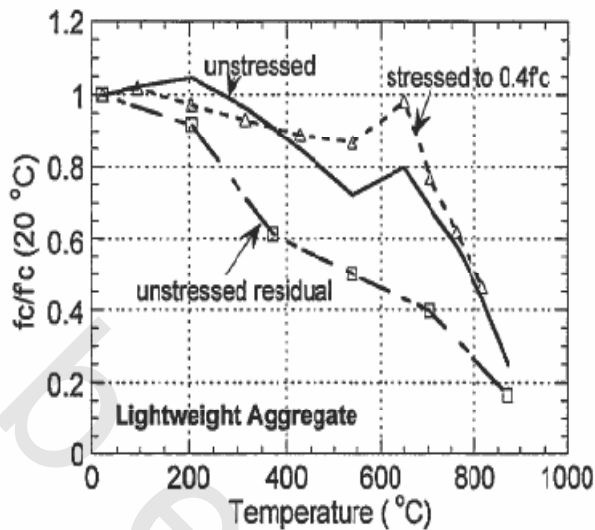
Fig. 2.24 High Temperature Models for HSC Concrete, [Kodur et al. 2008].

2.5.1 Experimental results on strength of concrete under high temperatures.

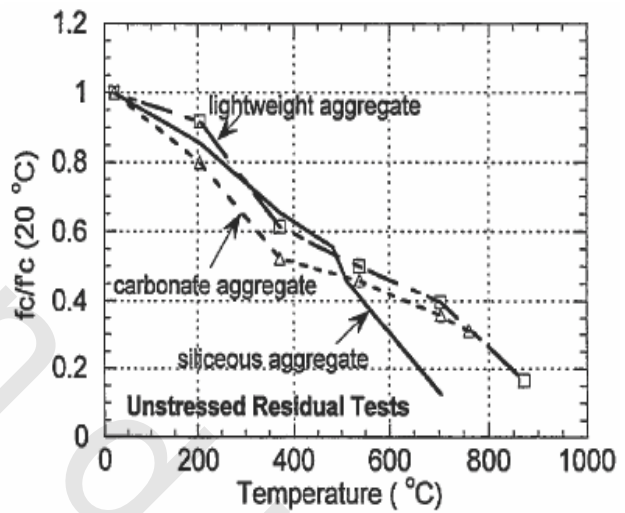
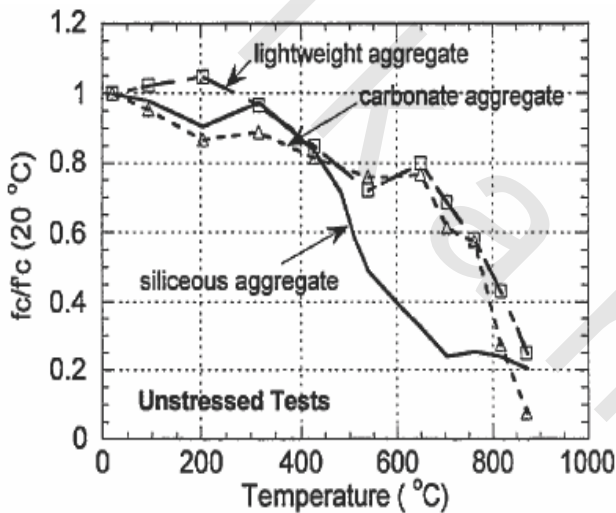
[Abrams, 1971] conducted a study of four variables including aggregate types (carbonatedolomite sand and gravel, siliceous, and expanded shale lightweight aggregates), testing methods (unstressed, stressed and unstressed residual experiments), concrete strengths (ranging from 22.8 MPa to 44.8 MPa), and temperatures (from 93°C to 871°C). The specimens were 75 mm × 150 mm cylinders. Abrams’ test data are important because they were used as a main reference in the current ACI design code for concrete under high temperatures.



(a) Carbonate aggregate concrete. (b) Siliceous aggregate concrete.



(c) Lightweight aggregate concrete.(d) Stressed tests.



(e) Unstressed tests.(f) Unstressed residual tests.

Fig. 2.25-Hot isothermal test results obtained by [Abrams ,1971].

Fig. 2.25 summarizes the test results. Up to about 480°C, all three concretes exhibited similar strength loss characteristics under each test condition (stressed, unstressed, and unstressed residual). Above 480°C, the siliceous aggregate concrete had greater strength loss and retained less strength for all three test conditions. Specimens made of carbonate aggregates and lightweight aggregates behaved about the same over the entire temperature range and retained more than 75 percent of their original strength at temperatures up to 649°C in unstressed tests.

For the siliceous aggregate, the strength was 75 percent of the original strength at 430°C. Compressive strengths of specimens with preload (stressed tests) were generally 5 percent

to 25percent higher than those without preload (unstressed tests). This may be due to the possibilitythat the preload helps to close existing cracks in concrete. The unstressed residual specimens had the lowest strengthcompared with the stressed and unstressed specimens tested at high temperatures. This isbecause the cooling of concrete actually generates very significant damage in concrete, as shownrecently by [Lee et al. 2008].

The test results of [Abrams,1971] indicate that strength recoverytook place only in a limited temperature range in the case of the stressed and unstressedexperiments.

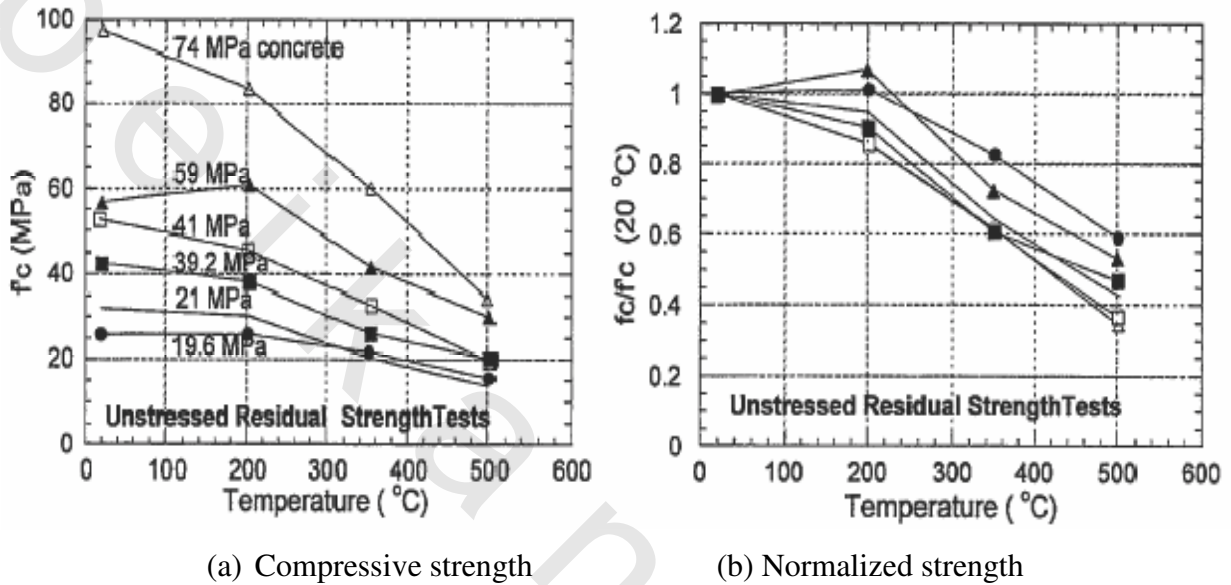
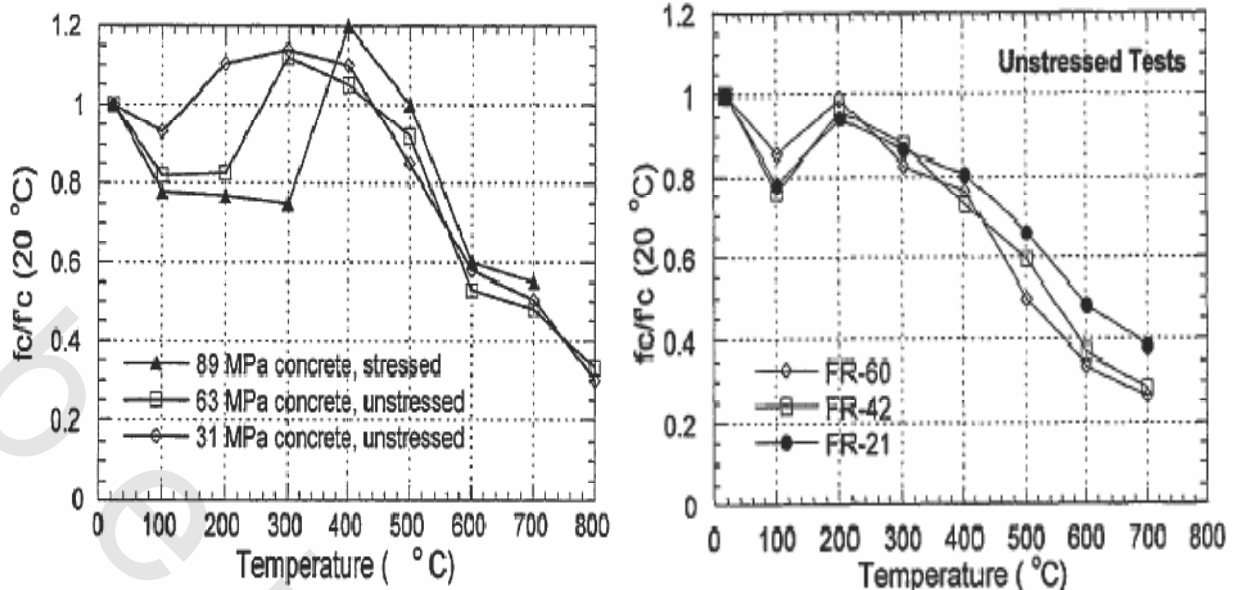


Fig. 2.26-Residual compressive strength obtained by [Morita et al. 1992].

[Morita et al. 1992] conducted unstressed residual strength tests as conducted in Fig. 2.26. The specimens were 100 mm \times 200 mm cylinders. The heating and cooling rate were 1 $^{\circ}\text{C}/\text{min}$ and target temperatures were 200 $^{\circ}\text{C}$, 350 $^{\circ}\text{C}$, and 500 $^{\circ}\text{C}$. The holding time at target temperatures to allow a steady state was 60 min. The test data showed that high strength concrete has higher rate of reduction in residual compressive strength.



(a)(b)

Fig. 2.27-Compressive strength vs. Temperature under hot isothermal conditions by
 (a) **Castillo and Durani, 1990** and (b) **Furumura et al. 1995**.

The effect of elevated temperatures on concrete strength and load-deformation behavior of HighStrength Concrete (HSC) and Normal Strength Concrete (NSC) were investigated by [CastilloandDurani, 1990]. Type I Portland cement with natural river sand and crushed limestone were used for preparing the concrete specimens in the form of 51mm×102 mm cylinders. **Fig.2.27(a)** shows the test results. In the case of the stressed experiment, 40 percent of the ultimate compressive strength at room temperature was applied to the specimens and sustained during the heating period. In the unstressed experiment, when exposed to temperatures in the range of 100°C to 300°C, HSC showed a 15 percent to 20 percent loss of compressive strength, whereas the NSC showed almost no strength loss in the temperature range. HSC recovered its strength between 300°C and 400°C, reaching a maximum value of 8 percent to 13 percent above the strength at room temperature. At temperature above 400°C, HSC progressively lost its compressive strength which dropped to about 30 percent of the room temperature strength at 800 °C. The trend of NSC was similar to that of HSC. [Furumura et al. 1995] performed unstressed tests and unstressed residual tests on 50 mm×100 mm concrete cylinders using three compressive strength levels: 21 MPa (normal strength concrete FR-21), 42 MPa (intermediate strength concrete FR-42), and 60 MPa (high strength concrete FR-60). The heating rate was 1°C/min and target temperatures were from 100°C to 700°C with an increment of 100°C. The time at target temperatures to allow a steady state was two hours. The concrete was made from ordinary

Portland cement. They observed that, for the unstressed tests, the compressive strength decreased at 100°C, recovered to room temperature strength at 200°C and then decreased monotonically with increasing temperature beyond 200°C as seen in Fig. 2.27(b). For the unstressed residual tests, the compressive strength decreased gradually with increasing temperature for the entire temperature range without any recovery.

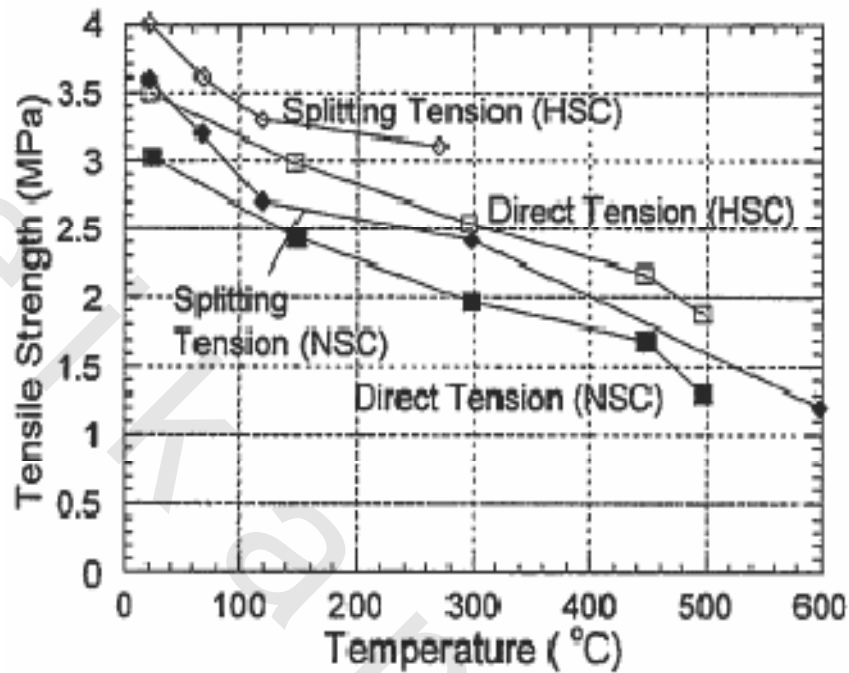


Fig. 2.28-Unstressed residual tensile strength obtained by [Noumowe et al. 1996].

[Noumowe et al ,1996] conducted unstressed residual strength tests to compare the performance of HSC exposed to high temperatures with NSC. The specimens were 160 mm×320 mm cylinders and 100 mm×100 mm×400 mm prisms. Normal strength concrete (38.1 MPa) and high strength concrete (61.1 MPa) were used. The prismatic specimens had enlarged ends and were used to measure tensile strength. Calcareous aggregates were used for both concretes. The specimens were heated at a rate of 1°C/min to target temperatures of 150°C, 300°C, 450°C, 500°C, and 600°C, which was maintained for one hour, and then allowed to cool at 1°C/min to room temperature. Uniaxial compressive tests, splitting tensile tests, and direct tensile tests were performed to obtain residual compressive strength, modulus of elasticity, and residual tensile strength versus temperature relationships. Fig. 2.28 shows the residual tensile strength relationship. Residual tensile strengths for NSC and HSC decreased similarly and almost linearly with increase of temperature. Tensile strengths of HSC at all temperatures were 15

percent higher than those of NSC. Also, the tensile strengths measured by splitting tension experiments were higher than those obtained in direct tension.

2.5.2 The effect of pre-loading on strength of concrete under high temperatures.

Preloading during heating has positive effects on both compressive strength and modulus of elasticity of concrete. **Fig. 2.29** demonstrates the positive effects (measured in the ‘hot’ state for unsealed CRT HITECO ultra-high performance concrete). Comparison of **Fig. 2.18 (a)** and **(b)** shows that the compressive strength and modulus of elasticity of the specimen under sustained loading is larger than those of specimens without the sustained loading. This aspect can be explained from the fact that compressive preloading inhibits crack development – although this explanation has not been fully validated.

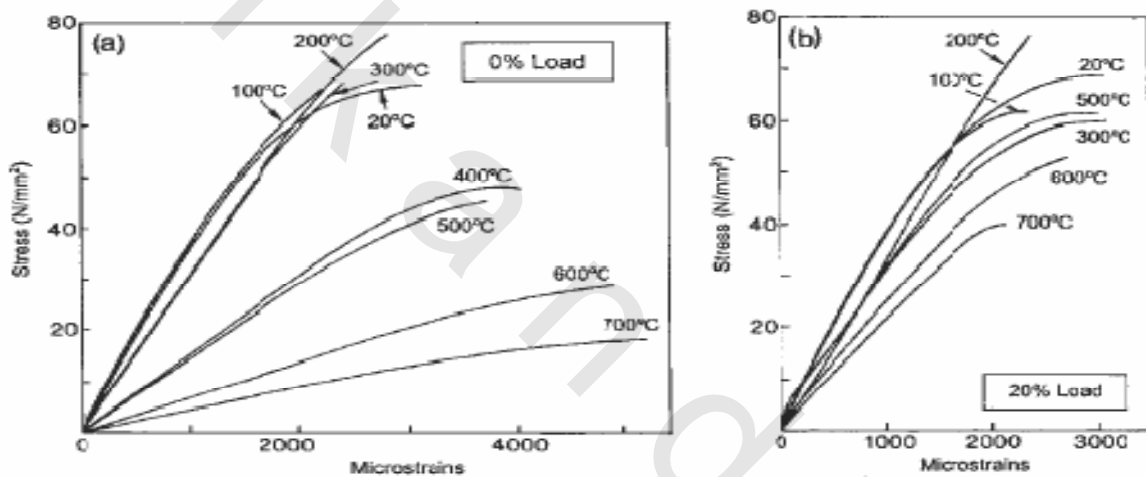


Fig. 2.29-The effects of loading and temperature during heating in uniaxial compression of unsealed concrete specimens [Khoury, 2002].

Fig. 2.30 [Khoury, 2002] shows the positive effect of temperature upon the residual (after cooling) compressive strength and the elastic modulus of unsealed C70 HITECO concrete containing thermally stable Gabbro Finnish aggregate. The specimens were heat cycled at 2°C/min under 0 percent and 20 percent of preload in compression, respectively. The results are shown in terms of percentage of strength and elastic modulus prior to heating. The figure shows the down-up-down trend of compressive strength as well as the increase of compressive strength with 20% preloading. It also shows the enhancement of stiffness with the 20% preloading.

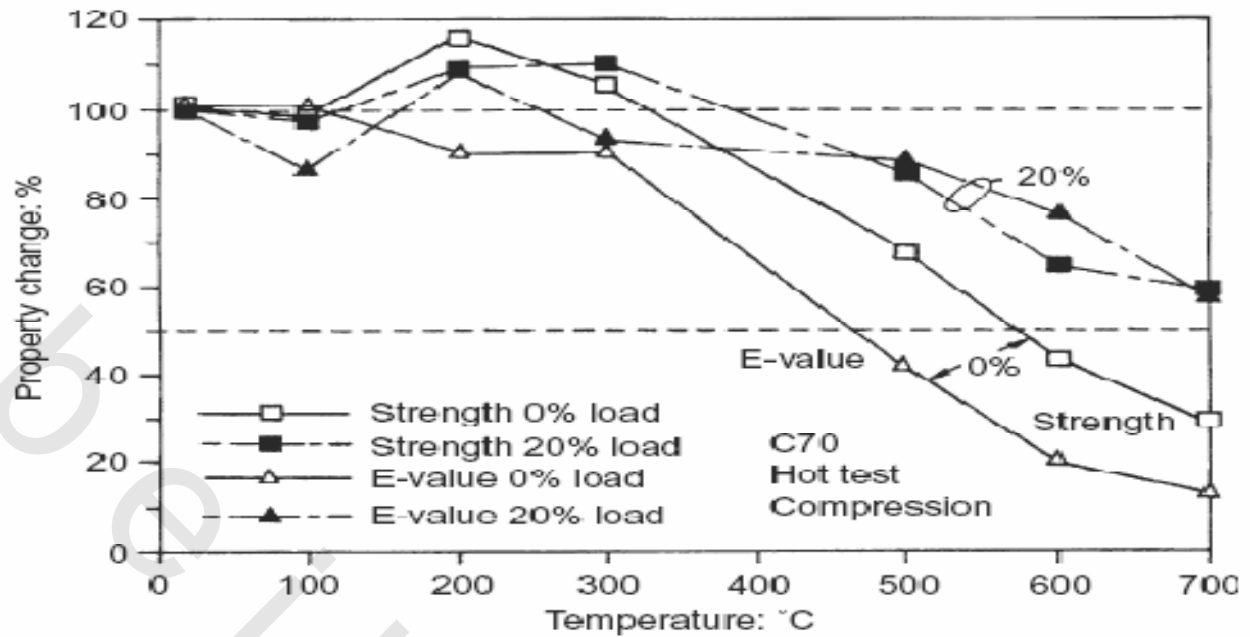


Fig. 2.30 Effect of temperature upon the residual (after cooling) compressive strength and elastic modulus of unsealed C70 HITECO Concrete -20 percent load: expressed as a percentage of strength prior to heating [Khoury, 2002].

2.6 Stiffness of concrete under high temperatures.

2.6.1 Experimental results on stiffness of concrete under high temperatures.

Similar to compressive strength of concrete, stiffness of concrete also decreases with increasing temperature. [Castillo and Durani, 1990] conducted tests to determine modulus of elasticity of HSC and NSC under hot condition where the modulus decreased by 5 to 10 percent in the temperature range of 100°C to 300°C as seen Fig. 2.31. Beyond 300°C, the elastic modulus decreased at a faster rate with increase in temperature. At 800°C, the elastic modulus was only 20 to 25 percent of the value at room temperature. [Morita et al. 1992] observed that high strength concrete have higher rate of reduction in modulus of elasticity than normal strength concrete after being exposed to temperatures up to 500°C where the specimens of 100 mm x 200 mm cylinders were tested under unstressed residual conditions (Fig. 2.32 (a) and (b)). [Noumowe et al, 1996] conducted residual modulus of elasticity of NSC and HSC where the modulus remained approximately 10 percent to 25 percent higher than those of NSC for entire temperature range (Fig. 2.32(c)). [Furumura et al. 1995] performed unstressed residual modulus of elasticity tests using three compressive strength levels. He observed the modulus of elasticity, in general, decreased gradually with increase of temperature. Fig. 2.32(d) shows the test results.

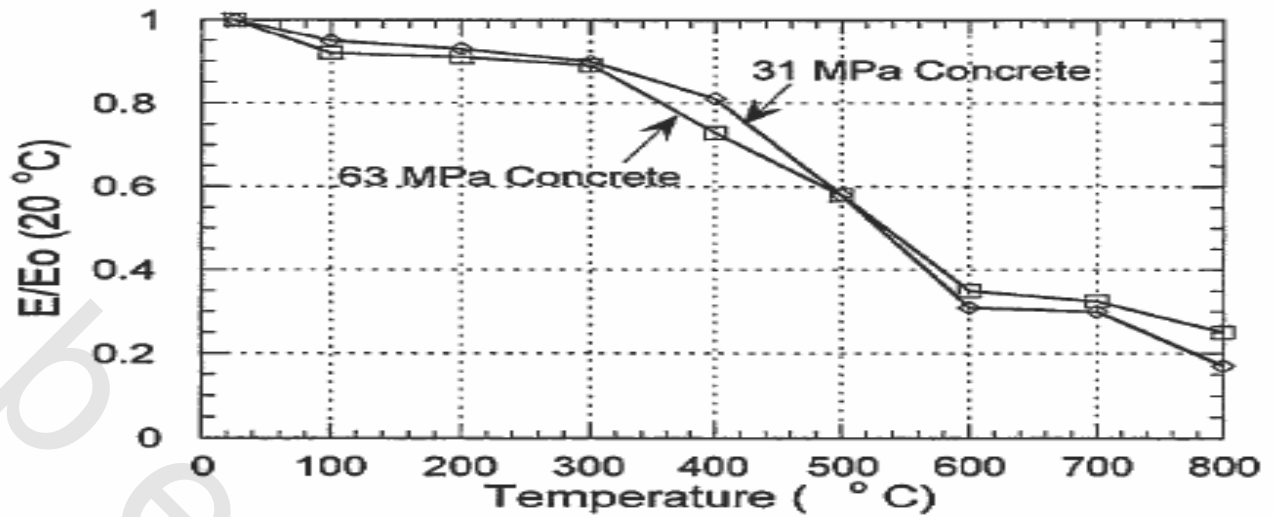
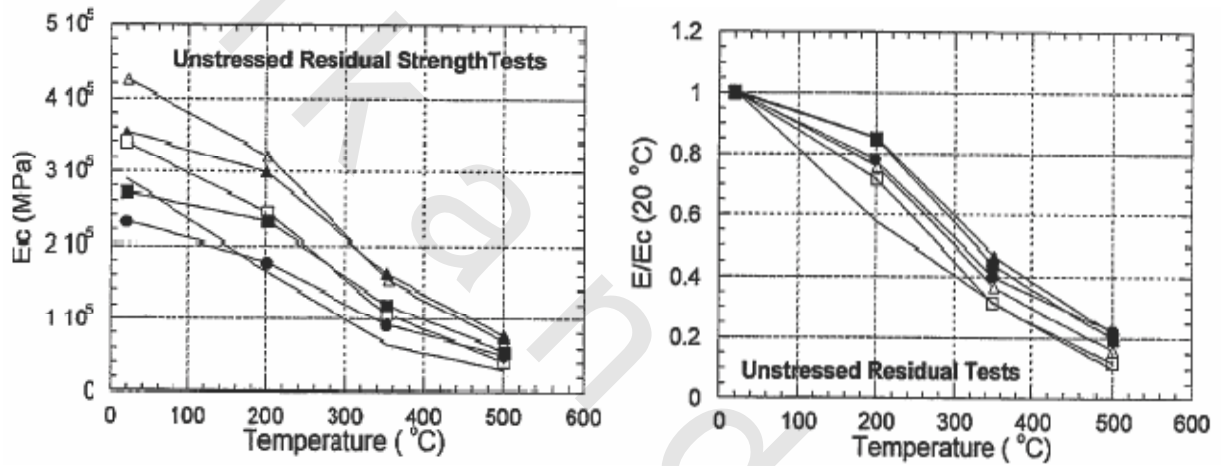
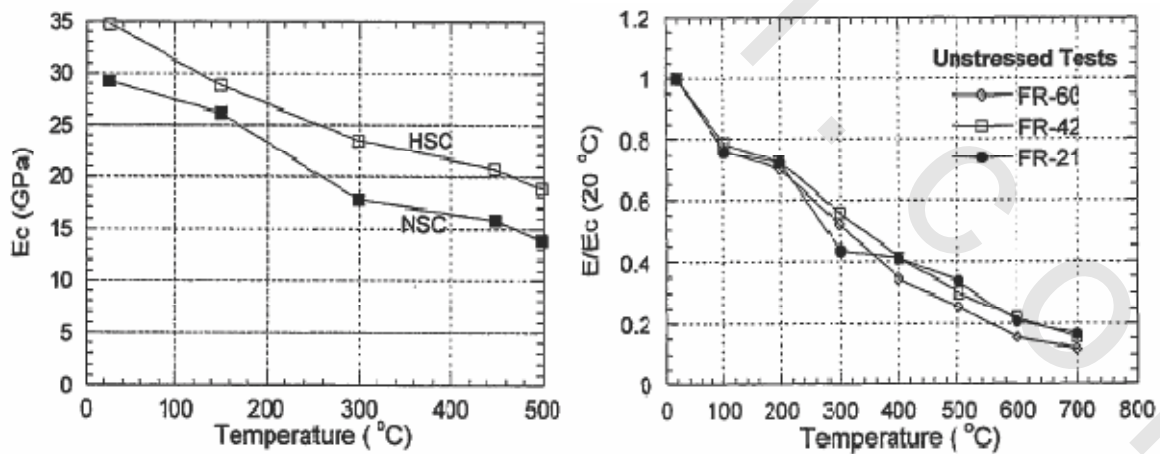


Fig. 2.31 Modulus of Elasticity under hot conditions by [Castillo and Durani, 1990].



(a) Residual elastic modulus. (b) Residual normalized elastic modulus.



(c) Residual elastic moduli for HSC and NSC. (d) Normalized elastic Modulus of HSC and NSC.

Fig. 2.32 Hot isothermal test results obtained by (a), (b) Morita et al., 1992 and (c) Noumowe et al., 1996, and (d) Furumura et al., 1995.

Fig. 2.33 shows the effect of cooling methods on modulus of elasticity of concrete. The slow cooling, means cools the specimens in a chamber at the rate of 1°C/min. from the targeted temperatures down to room temperature; the natural cooling means cooling the specimens under room temperature; and the fast cooling stands for cooling of specimens in a water tank. Test data showed that the water cooling (fast cooling) resulted in the largest reduction in the stiffness of concrete. This is due to the fact that there is a steep thermal gradient in the concrete during the fast cooling which causes more damage than the natural and slow cooling methods.

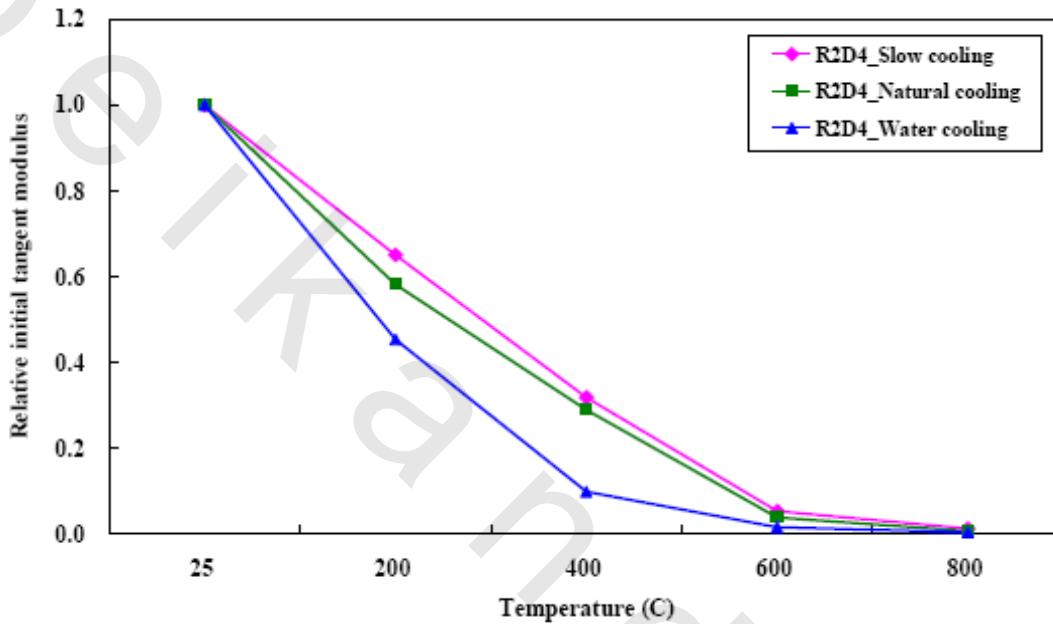
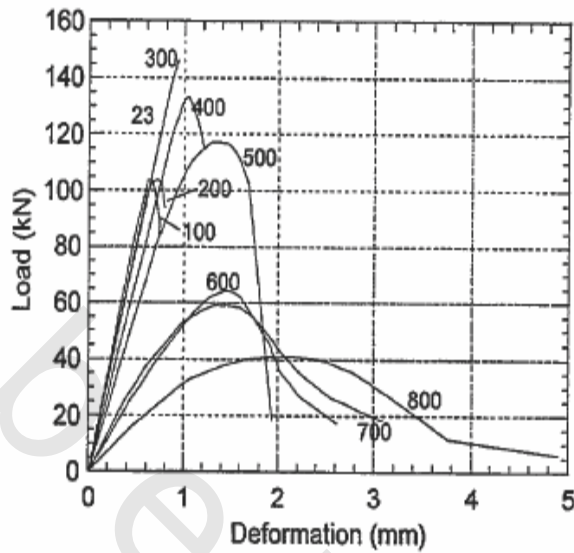


Fig. 2.33-The effect of cooling methods on modulus of elasticity of concrete [Lee et al. 2008].

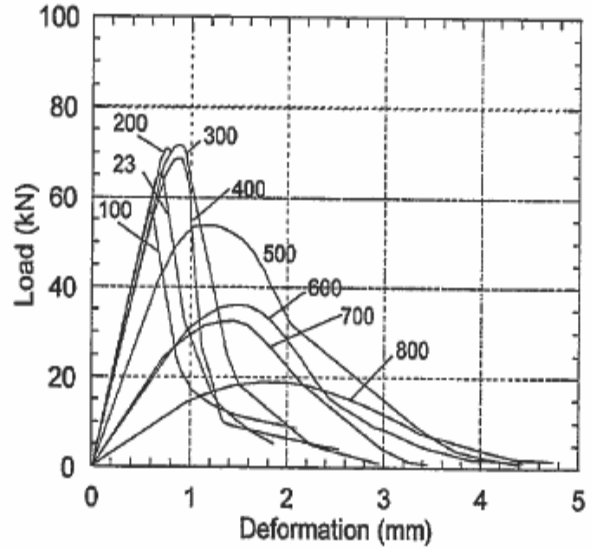
2.7 Stress-strain relations of concrete under high temperatures

2.7.1 Stress-strain of concrete under high temperatures

The load-deformation plots for HSC and NSC are shown in **Fig. 2.34 (a)** and **(b)** [Castillo and Durani, 1990]. NSC specimens did exhibit ductile failure except for 200°C. Between 300°C and 800°C, the NSC specimens were able to undergo large post-peak strains while the decrease in strength was more gradual. HSC showed brittle failure up to 300°C, and with further increasing temperature, the HSC specimens began to exhibit a more ductile failure. [Furumura et al., 1995] obtained stress-strain curves for concretes with different strengths, as shown in **Fig. 2.35 (a)** and **(b)**. HSC exhibited steeper slopes than the NSC at temperature up to 300°C to 400°C in the unstressed test.

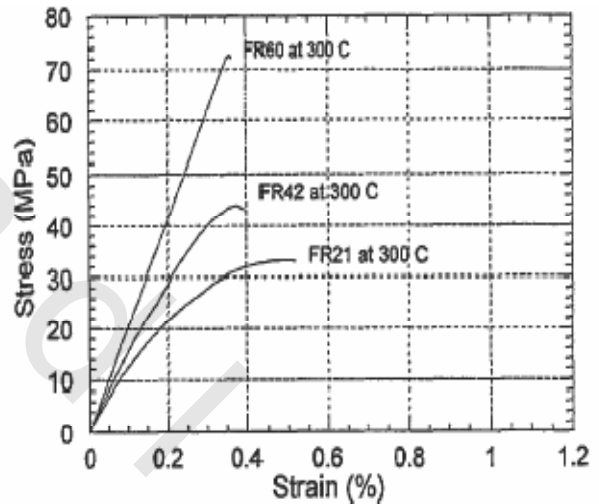
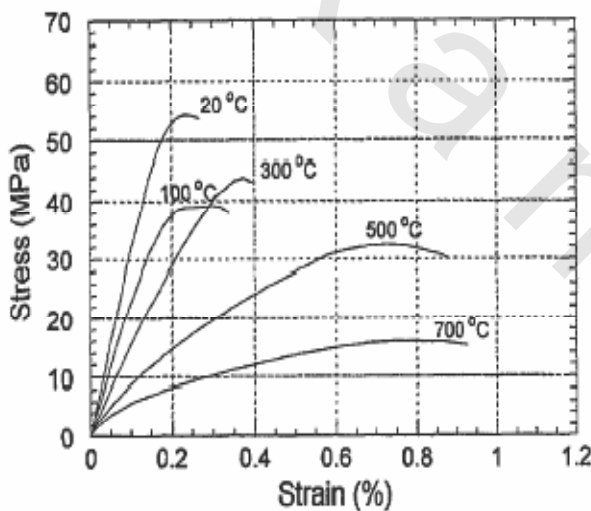


(a) Load-deformation of HST



(b) Load-deformation of NSC

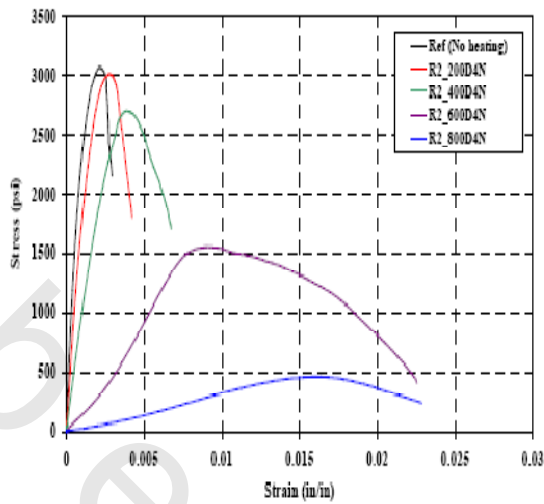
Fig. 2.34- Hot isothermal test results obtained by [Castillo and Durani, 1990].



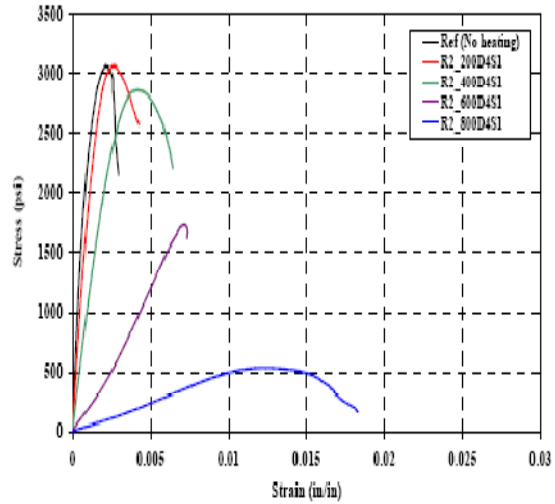
(a) Stress-strain curves (FR-42) (b) Stress-strain curves at 300°C

Fig. 2.35- Hot isothermal test results obtained by [Furumura et al. 1995].

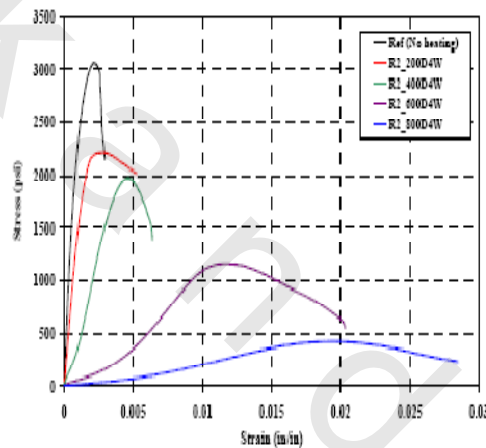
Fig. 2.36 shows the effect of cooling methods on stress-strain curve of concrete [Lee et al. 2008]. Comparing the test data of normal cooling and fast (water) cooling, one can clearly see that both the peak stress (the strength) and the initial slope (the stiffness) of the curves of fast cooling method are lower than those obtained by normal cooling. Therefore, it can be concluded that fast cooling has adverse effect on both strength and stiffness of the concrete.



(1) Normal cooling



(2) Slow cooling



(3) Fast (water) cooling

Fig. 2.36-Stress-strain curves of concrete specimens by (1) normal cooling, (2) slow cooling, and (3) fast (water) cooling after heating to 200, 400, 600, and 800 °C [Lee et al. 2008].

2.8 Thermal expansion of concrete under high temperatures.

Free thermal strain of concrete is defined as the strain of concrete induced by heating without loading and drying. Free thermal expansion of concrete is usually measured under a saturated state to avoid the drying effect. In a typical test for thermal expansion of concrete, a concrete specimen is submerged in a water tank and the change in the length of the specimen is measured while the water temperature rises to a target level (see AASHTO TP60-00). Under this special condition, both cement paste and aggregate expand with increasing temperature. However, this is not a valid testing method when the environmental temperature is higher than 100 °C

since water starts to evaporate and cannot be used as the testing media. Furthermore, it is not the actual situation for a real concrete structure under service condition or under an accidental condition, where both heating and drying take place at the same time and thus the coupling effect must be taken into account.

Thermal expansion of concrete is mainly affected by the type and the amount of aggregate. An average value for the coefficient of thermal expansion of concrete is about 10 millionths per degree Celsius ($10 \times 10^{-6}/^{\circ}\text{C}$ or $6 \times 10^{-6}/^{\circ}\text{F}$), although the value ranges from $6 \times 10^{-6}/^{\circ}\text{C}$ to $13 \times 10^{-6}/^{\circ}\text{C}$. **Table 2.3** shows some experimental results on the coefficient of thermal expansion of concretes made with aggregates of various types. These data were obtained from tests on small concrete specimens in which all factors were kept the same except aggregate type. In each case, the fine aggregate was made of the same material as the coarse aggregate.

Table 2.3 Coefficient thermal expansion of some types of aggregate.

Aggregate type	Coefficient of thermal expansion millionths per $^{\circ}\text{C}$
Quartz	11.9
Sandstone	11.7
Gravel	10.8
Granite	9.5
Basalt	8.6
Limestone	6.8

Coefficient of thermal expansion of concrete is temperature dependent and its temperature dependent behavior is highly nonlinear. Assuming all other influential parameters remain constants except temperature, the relationship between thermal strains and temperature is shown in **Fig. 2.37**, which was developed by [Nielsen, Pearce and Bicanic] (2004). The thermal strain increases with temperature up to $T = 620^{\circ}\text{C}$ and beyond which it is assumed to remain constant. The coefficient of thermal expansion corresponding to **Fig. 2.37** is a function of temperature as illustrated in **Fig. 2.38**. One can see from **Fig. 2.38** that under low temperature range (e.g. from $20 - 120^{\circ}\text{C}$), the variation of α (coefficient of thermal expansion) is not large, and thus α can be considered as a constant under room temperature.

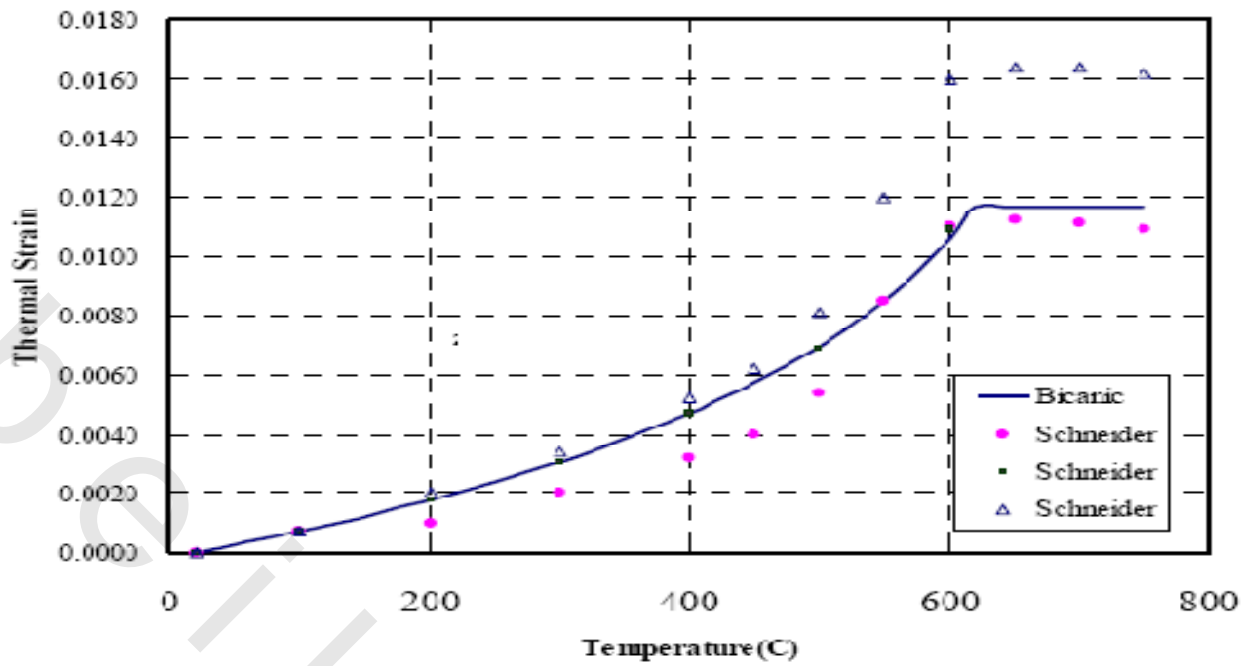


Fig. 2.37-Thermal strain of concrete vs.temperature.

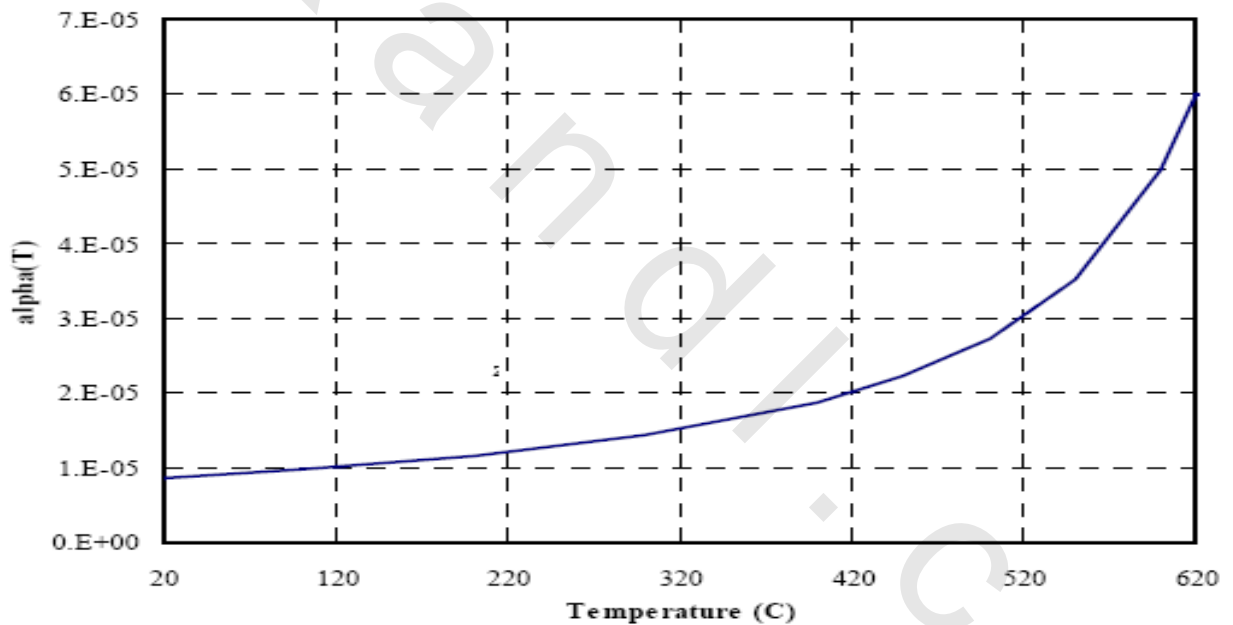


Fig. 2.38-Coefficient of thermalexpansion of concrete vs. temperature.

The expressions below are for the thermal strain and coefficient of thermal expansion shown in **Figs. 2.37** and **2.38**. They consider the temperature dependence of the thermal expansion in an incremental format (thermo-hypo-elasticity):

$$\dot{\varepsilon}_{th} = \alpha(T) \dot{T}$$

$$\varepsilon_{th} = -6 \times 10^{-3} \ln \left[1 - \frac{\theta}{7} \right]$$

$$\alpha = \frac{6 \times 10^{-5}}{7 - \theta} \quad 0 \leq \theta \leq 6, \quad \theta = \frac{T - T_0}{100}$$

2.9 Shrinkage of concrete under high temperatures.

Shrinkage of concrete is defined as long-term strain of concrete due to drying without loading and heating. Shrinkage tests performed under different temperatures will result in different results. **Fig. 2.39** shows the test data from [Schneider, 2002]. One can see that the shrinkage of concrete at 60°C is actually higher than those at 110°C and 140°C.

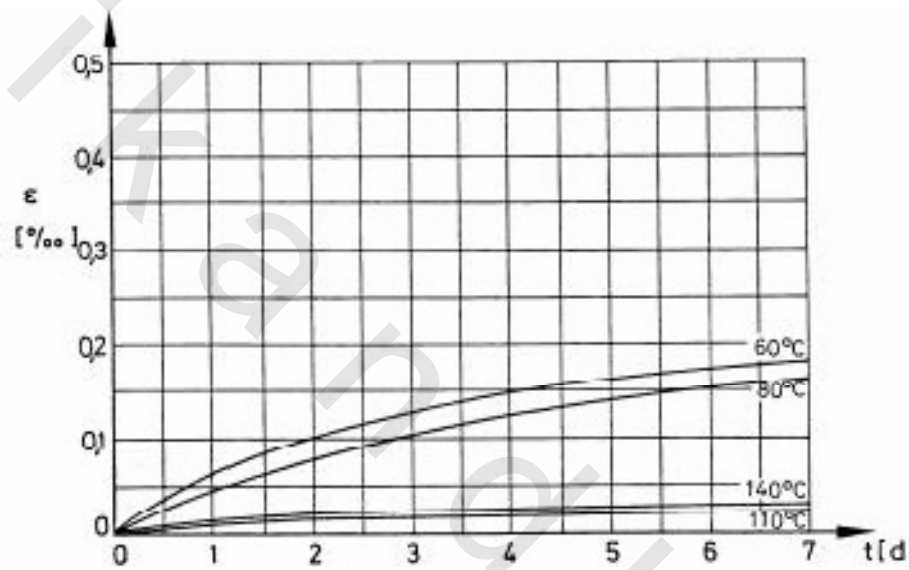


Fig 2.39-Shrinkage of concrete under different temperatures [Schneider, 2002].

There are many shrinkage models for concrete under room temperature. Since the shrinkage of concrete is induced by moisture loss, therefore, most of the models are related to diffusion theory of moisture in concrete, which will not be described in this report. For the shrinkage of concrete under high temperature, however, there has been not much research. Shrinkage of concrete is coupled with creep and mechanical loading under elevated temperatures, which will be described in the next section. Some empirical values for shrinkage of concrete were suggested by [Schneider, 2002].

- limestone concrete: 20-100 °C; $e_s = 200$ to $300 \cdot 10^{-6}$
- limestone concrete: ~ 80 °C; $e_s = 300$ to $400 \cdot 10^{-6}$
- quartzite concrete: 20-100 °C; $e_s = 200$ to $450 \cdot 10^{-6}$
- limestone concrete: ~ 150 °C; $e_s = 500 \cdot 10^{-6}$
- limestone concrete: 150-350 °C; $e_s = 800 \cdot 10^{-6}$

2.10 Spalling of concrete under high temperatures.

Spalling is the breaking off of pieces of concrete from the surface of the structure when it is heated due to thermal stresses or high pore pressures or both. The fire resistance of concrete assumes that all concrete remains in place during the fire event. The beneficial properties of concrete in a fire are reduced if concrete spalls during elevated temperatures. The spalling phenomenon is not well understood but conventional theory states that spalling is chiefly caused by the increase in water vapor during elevated temperatures. If the concrete cannot naturally dissipate the pressure increase due to the increase in water vapor, the pressure exceeds the tensile strength of the concrete and spalling occurs. It could be related to a difference in the coefficient of thermal expansion of the aggregate relative to the cement paste. In that sense, carbonate aggregates are more compatible with cement paste than siliceous aggregate. In some cases, the chance of spalling can be reduced based on the choice of aggregate. High strength concrete tends to be more susceptible to spalling due to its reduced pore volume and low diffusion of water vapor during elevated temperatures. Lightweight concrete is less susceptible to spalling due to its increased permeability, which allows water vapor to expand into voids, thus relieving internal stresses. The behavior of spalling is very difficult to predict although large amount of researches have been carried out into it.

[Connolly 1995] presented the categorization suggested by [Gary, 2010] that spalling can be grouped as follows:

- a) Aggregate spalling, which is defined as a splitting of aggregates at the heated surface. This spalling occurs to areas on the heated surface within the first 20 minutes of exposure to the standard heating test with maximum depth of their moved section of about 5 to 10 mm. Aggregate spalling has minor effect on the fire resistance of concrete structures.
- b) Corner spalling, which is defined as a gradual disintegration of parts of heated concrete at the corner of member such as beams and columns. This type of spalling occurs after 30 minutes of exposure to the standard test. Corner spalling attributed to the loss of tensile strength leading to bond failure. Fortunately, corner spalling can usually be repaired easily after fire.

- c) Surface spalling, which is defined as the violent removal of sizeable lumps from the heated surface up to 100x100 mm. The loss of sizeable parts of concrete means the effective area of concrete is reduced and the exposure of the steel-reinforcement to fire causes result in rapid rise of steel temperature. Therefore, the fire resistance of concrete structures decreases significantly.
- d) Explosive spalling, which is described as a very violent bursting of large parts of heated concrete. This type of spalling is extremely dangerous and may cause sudden and complete failure accompanied by a large release of energy and produces atypical explosive noise.

Concrete exposed to fire causes spalling of the concrete cover and exposure of the reinforcing steel. This exposure will definitely cause a reduction in the resistance strength of the reinforcing steel, and thus reduce the ultimate capacity of the structural element. The incorporation of synthetic fibers such as polypropylene fibers which melt at approximately 160°C during the fire to produce channels where steam can escape is recommended [Connolly 1995]. The permeability of concrete is considered as the main parameter influencing spalling. **Fig. 2.40-a** illustrates the situation in case the permeability is not sufficient to avoid spalling: water vapor, resulting from vaporization of evaporable water at temperatures above the vaporization temperature, i.e., $T > T_{\text{Vap}}$ (with $T_{\text{Vap}} \geq 100$ °C), flows toward the heated surface through the pore system of concrete characterized by “dry” conditions. On the other hand, water vapor flows further into the concrete structure. In regions characterized by $T \approx T_{\text{Vap}}$, the water vapor condenses again. This newly built water together with the evaporable water present in this region forms a saturated layer, acting as an impermeable wall for the gas flow (“moisture clog”, see **Fig. 2.40-c**). If the permeability of the “dry” zone of the concrete member is not sufficient to avoid a continuous pressure build-up in consequence of vaporization of evaporable water, spalling as indicated in **Fig. 2.40-d** occurs.

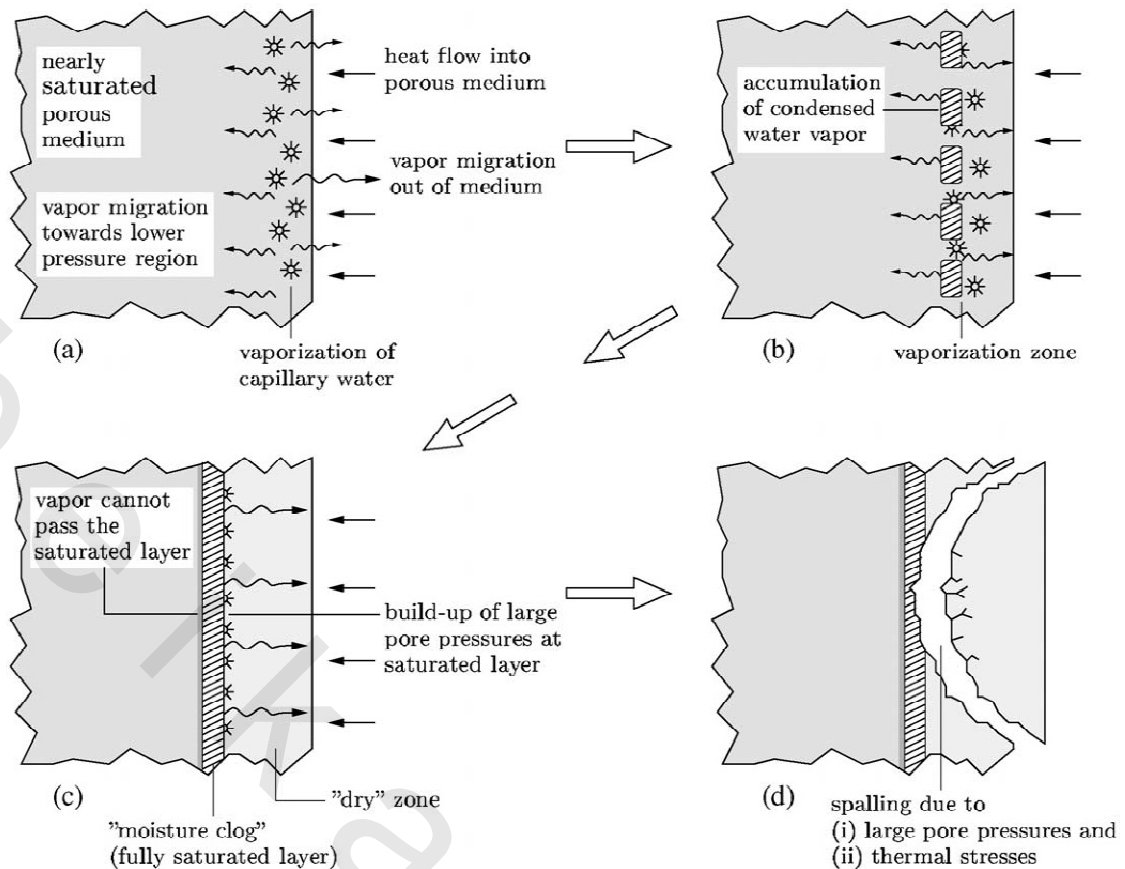


Fig. 2.40- Illustration of mechanism of spalling of concrete as a result of fire loading according to Refs. [Consolazio 1997 and Schneider, 2002].

2.11 Temperature Distribution Within the Concrete Members Exposed to a Standard Fire.

ACI-216 provides information on the temperature distribution in a number of concrete shapes during fire exposure. **Fig. 2.41 (a), (b), and (c)** show temperatures within concrete slabs during fire tests [Abrams and Gustafsson 1968]. Slab thickness did not significantly affect the temperatures except for very thin slabs or when the temperatures were less than about 400 F (200°C). Temperatures in slabs were obtained from specimens 3 x 3 ft (0.9 x 0.9 m) in plan with protected edges.

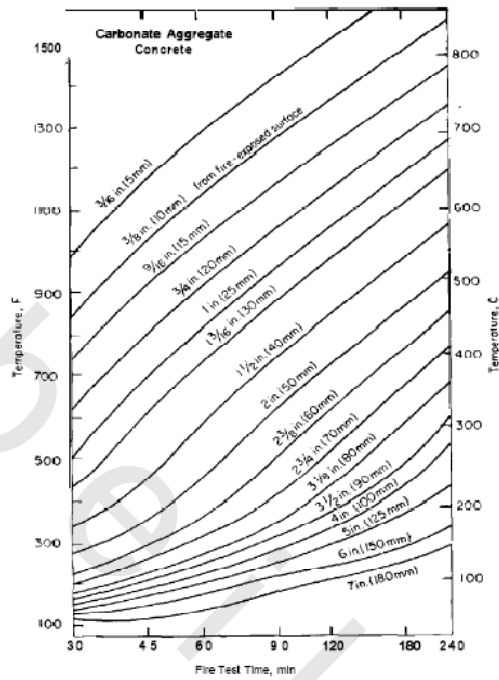


Fig. 2.41(a)-Temperature within slabs during fire tests carbonate aggregate concrete

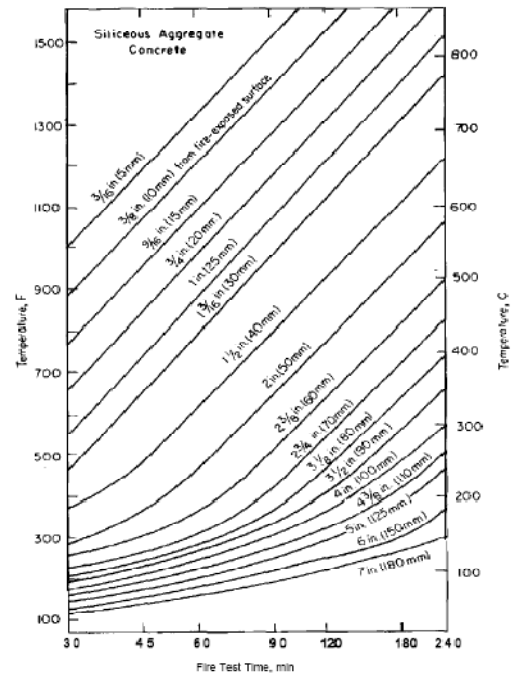


Fig. 2.41(b)-Temperatures within slabs during fire tests siliceous aggregate concrete

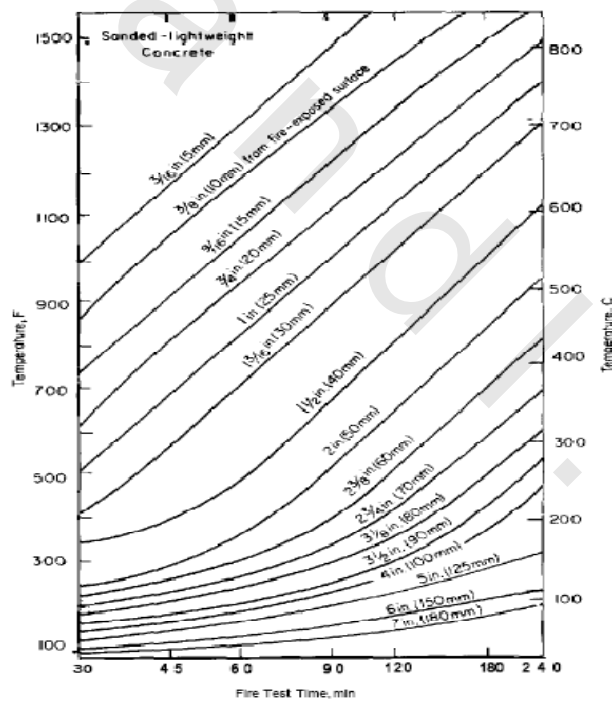


Fig. 2.41(c)-Temperatures within slabs during fire tests sanded lightweight concrete

Also Fig.2.42 (a, b, c) show temperature distributions in a 12in. (305 mm) wide rectangular carbonate aggregate concrete beam. Based on a numerical technique developed by [Lie and Harmathy, 1972] the temperature distribution in concrete-protected steel columns was analyzed, and an empirical formula was derived for the calculation of the fire endurance of such

columns [Lie and Harmathy, 1974]. Lie and Allen, in technical paper 378, studied the temperature distribution in solid concrete columns during fire. Lie and Lin conducted a series of 38 fire tests of full-sized reinforced concrete columns in the period from 1976 to 1986. These latter studies covered reinforced concrete beams as well.

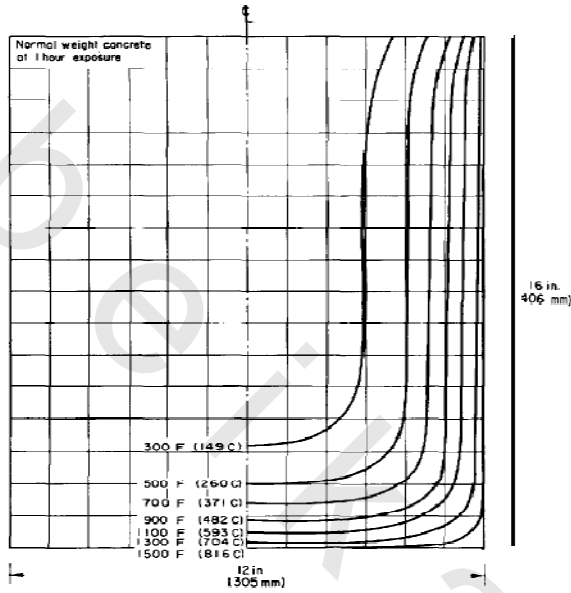


Fig. 2.42 (a) -Temperature distribution in normal weight concrete rectangular unit at 1 hr of fire exposure

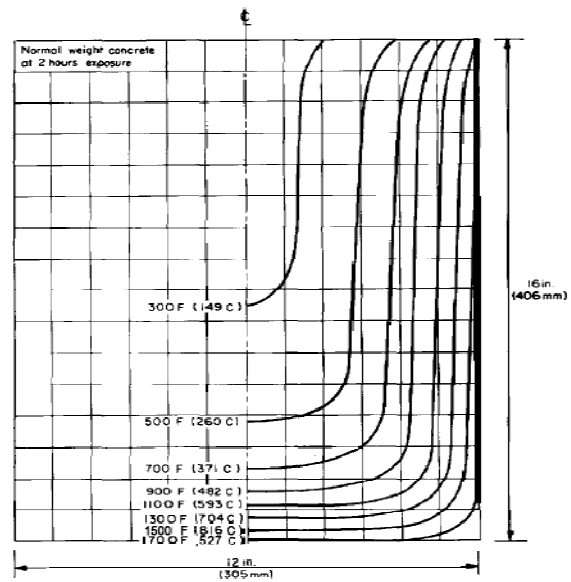


Fig. 2.42 (b) -Temperature distribution in normal weight rectangular unit at 2 hr of fire exposure

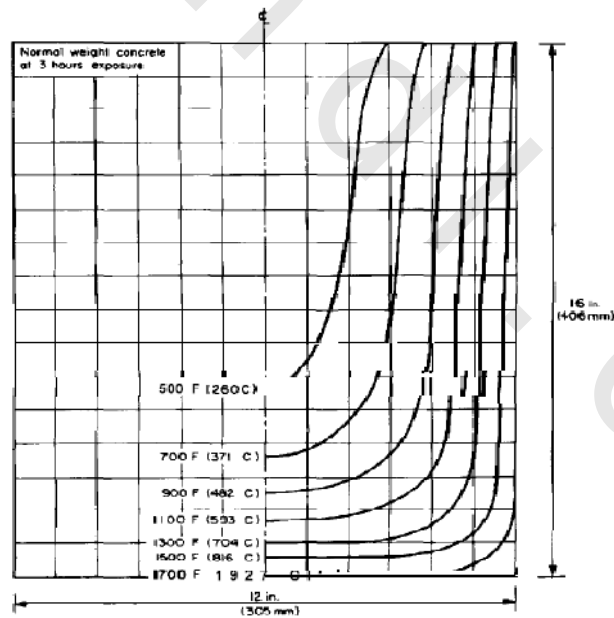


Fig. 2.42 (c) -Temperature distribution in normal weight rectangular unit at 3 hr of fire exposure

2.12 High-Temperature Performance of a HPFRC for Heavy-Duty Road Pavements.

A high-performance concrete reinforced with polymeric fibers ($f_c = 120$ MPa) is being developed for the construction of heavy-duty road pavements. All mechanical tests were performed in the laboratory of the structural engineering department of Milan University of Technology. After the thermal cycles, each specimen was tested in uniaxial compression and in three-point bending, to evaluate the compressive strength, the elastic modulus (secant, static) and the indirect tensile strength. The plots of f_c and E_c are shown in **Figs. 2.43** and **2.44**. Three tests were carried out for each reference temperature. A limited number of tests was performed in “thermal-shock” conditions, i.e. by introducing the cylinders into the furnace, previously heated to 600°C , and by keeping them at high temperature for 30'. No spalling occurred, but a net of hairlike cracks appeared on the surface of the specimens. On the contrary, two cylinders without fibers exploded 5'-10' after being put inside the furnace. The explosions broke the cylinders into three pieces, with the cracks localized in the cross sections, because of the combined effects of pore pressure and self-stresses. After being extracted from the furnace, the specimens were left to cool to room temperature and then were tested in uniaxial compression. The residual strength f_c^* turned out to be very close to that of the specimens slowly heated to 600°C ($f_c^* = 47.5$ MPa, see **Fig. 2.43**), this fact being totally unexpected, since the mechanical decay appears to be the same for slowly-heated and suddenly heated specimens. Should it be confirmed by further tests, the conclusion would be that the strength decay depends solely on the maximum temperature reached by the material, and not on the heating rate.

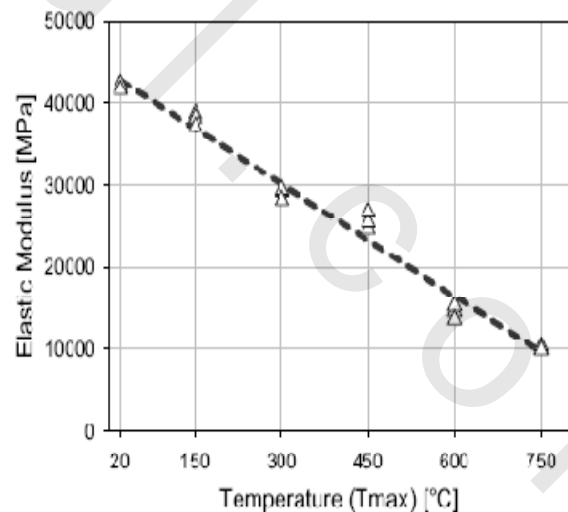
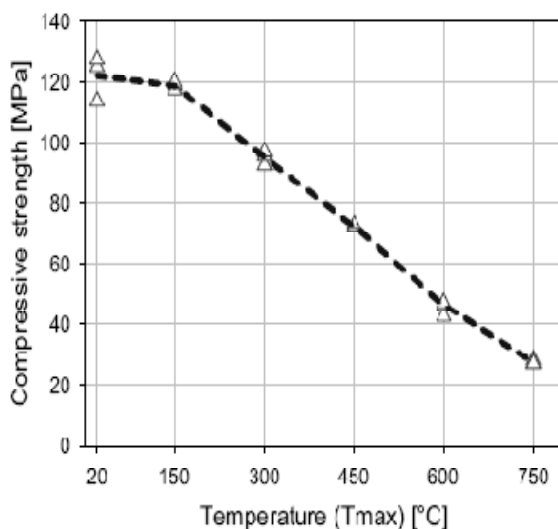


Fig. 2.43 - Residual compressive strength. **Fig. 2.44** - Residual elastic modulus.

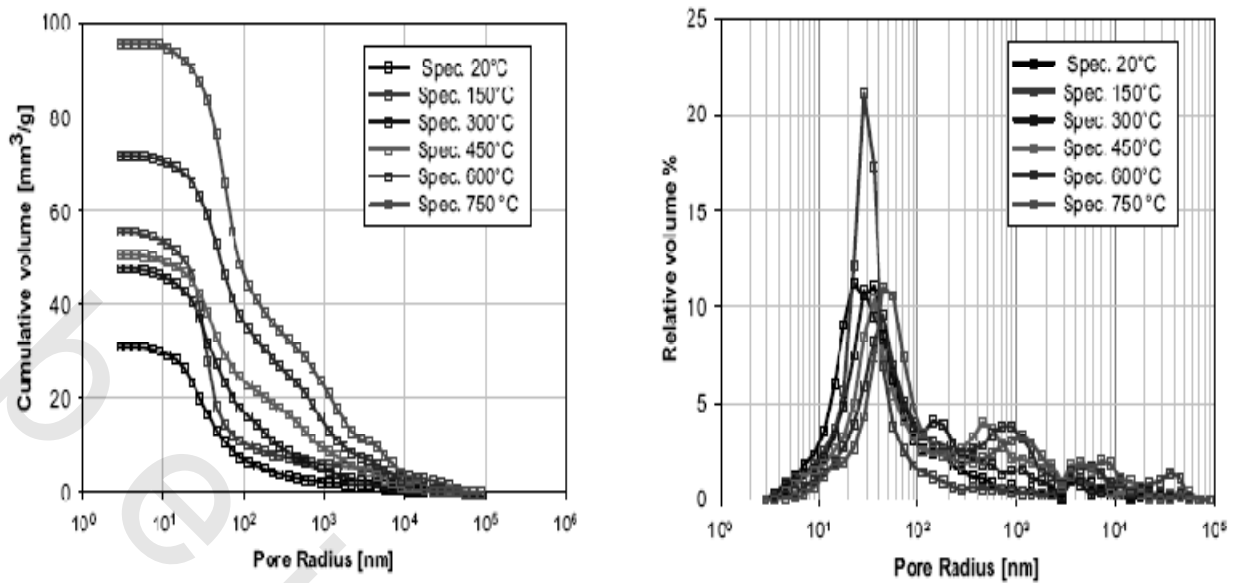


Fig. 2.45- Cumulative distribution of pore size.**Fig. 2.46-** Differential distribution of pore size.

Increasing with the maximum temperature as shown in **Fig. 2.45**, and the peak of the differential distribution were moved towards larger pore dimensions as the maximum temperature increases as presented in **Fig. 2.46**. The physical state of the polymeric fibers was studied by means of electron microscopy. Above 150°C, the fibers disappear, since they melt and vaporize, leaving an evident mark in the form of an oblong cavity **Fig. 2.47 (a, b)**.

Scanning electron microscopy was used also to investigate the formation and propagation of the micro-cracks. As shown in **Fig. 2.48**, discontinuous micro-cracks appear at 300°C; above this temperature, the micro-cracks become more numerous and wider ($T_{max} = 450^\circ\text{C}$). After the transition of quartz from the α - to the β -crystalline form ($T = 573^\circ\text{C}$), the micro-cracks exhibit a marked increase in both number and width, and some micro-cracks start crossing the aggregate particles. Finally, mercury porosimetry, and electron and optical microscopy give useful information on the damaged microstructure.

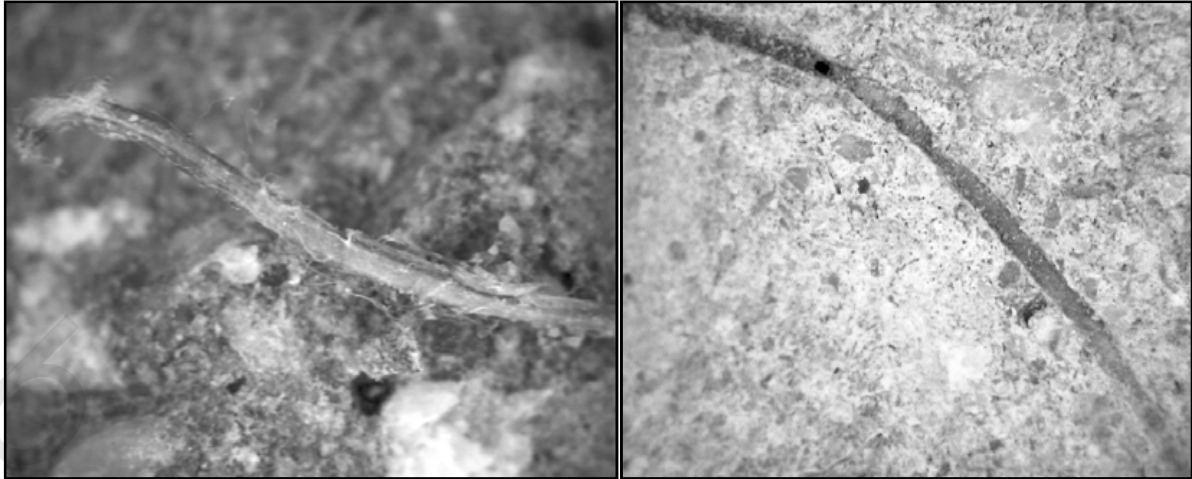
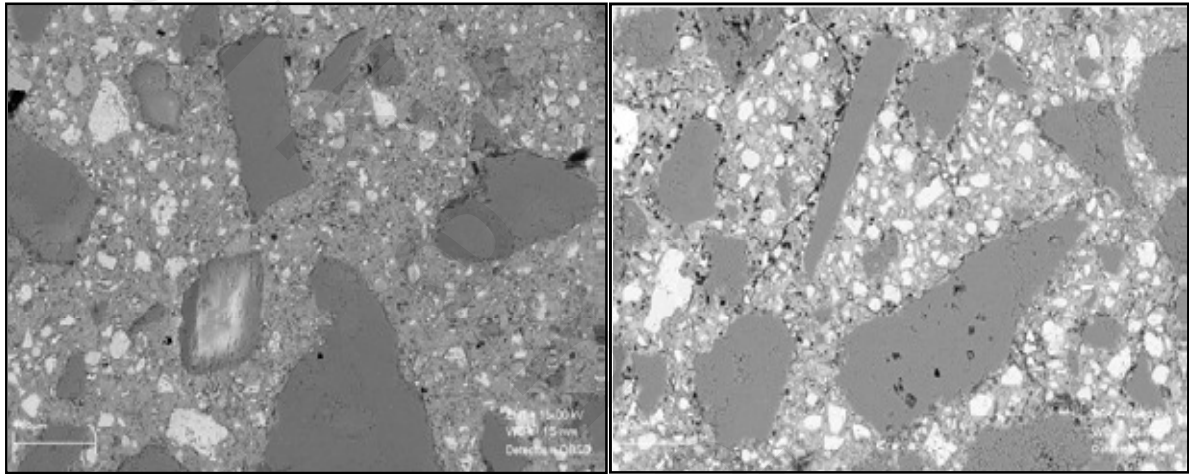


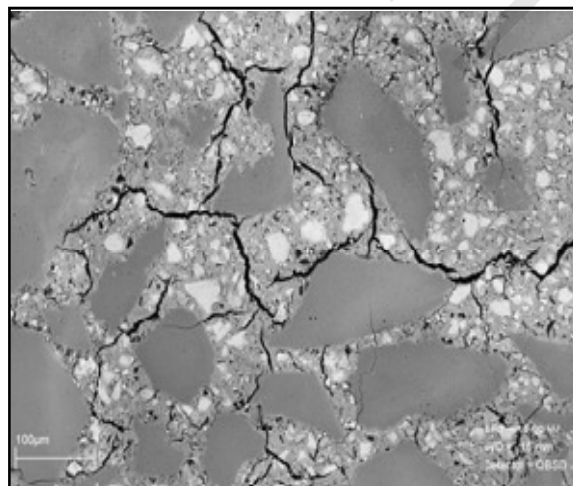
Fig. 2.47 (a)- After heating to 150°C, the fibers are still there (melting temp. \approx 150-170°C).of the fibers is left.

Fig. 2.47 (b) - After heating to 300°C, only the mark



$T_{max} = 20\text{ }^{\circ}\text{C}$

$T_{max} = 300\text{ }^{\circ}\text{C}$



$T_{max} = 600\text{ }^{\circ}\text{C}$

Fig. 2.48 - Evolution of the micro-cracks in the specimens first slowly heated to high temperature and then cooled to room temperature.

2.13 Limestone powder.

Limestone, when ground for optimum fineness, can lower the water demand, reduce bleeding, improve workability, and increase strength because it improves overall particle gradation of a cement (Schmidt 1992). In general the use of 15% to 20% limestone can result in optimal packing density; however this is less pronounced in cements that are finer [Schmidt et al. 1994]. When the clinker and limestone are interground, the limestone is normally easier to grind and tends to become the majority of the smaller particles (Fig. 2.49), thus broadening the particle size distribution. When ground separately the limestone needs to be sufficiently fine since if it is too coarse, an increase in particle spacing may occur along with an increase in the voids between the particles. This can result in increased water absorption and reduced strength [Cam and Neithalath 2010]. Some researchers have suggested a potential benefit of intergrinding on the carboaluminate reaction, for example to reduce porosity slightly [Matschei et al. 2007a] and thereby improve durability.

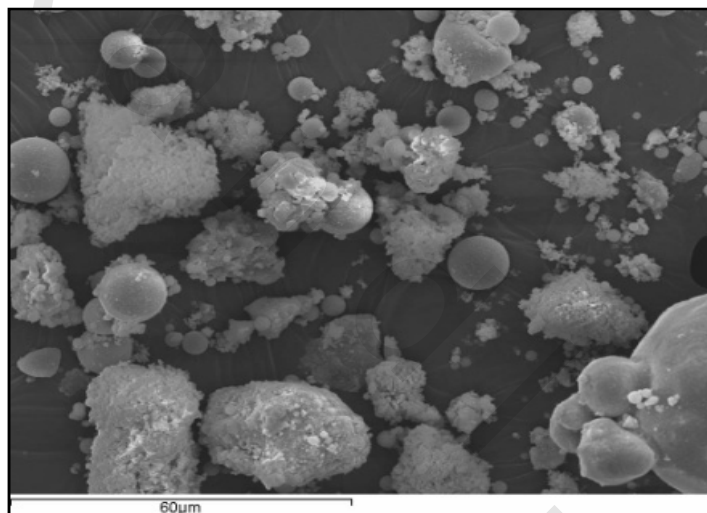


Fig. 2.49 Raw materials of limestone powder

2.14 Bentonite.

Bentonite is essentially highly plastic clay containing not less than 85% clay mineral, montmorillonite. A great commercial importance is attached with bentonite which possesses inherent bleaching properties like fuller's earth. Hence, it is known as bleaching clay. There are two types of bentonites; namely, swelling-type or sodium bentonite and non-swelling-type or calcium bentonite. Sodium bentonite is usually referred to as bentonite, whereas calcium bentonite is called Fuller's earth. The commercial importance of bentonite depends more on its physicochemical properties rather than its chemical composition. Excellent plasticity and

lubricity, high dry-bonding strength, high shear and compressive strength, low permeability and low compressibility make bentonite commercially viable.

Bentonite range in colour from black through to white but most frequently are bluish-green when fresh, weathering to a yellowish-brown colour at or near outcrop due to the oxidation of ferrous iron.

The composition of some bentonite among the most contents is montmorillonite. Montmorillonite is a mineral that contains compounds $Al_2O_3 \cdot 4Si \cdot H_2O$ [Wijaya and J. D. S. Rohman, 2008], other minerals contained in the bentonite is Mg and Ca occasionally. Bentonite lattice structures composed of a single plate located between two Al_2O_3 SiO_2 plates. Since the structure is montmorillonite can expand and contract, and have the power of water and cation adsorption higher.

2.15 How PP fibres inhibit explosive spalling

The addition of suitable polypropylene monofilament micro-fibers as shown in Fig 2.50 to counteract explosive spalling in cast concrete [Ali et al, 1996] and in shotcrete has been accepted for many years, but to design an optimized micro-fiber to prevent explosive spalling, it is necessary to have an understanding of the detailed mechanism by which these fibers function. Since the spalling is caused by pressure created by a restriction on the movement of moisture or steam, then somehow the presence of the fibers must relieve that pressure.



Fig 2.50-Polypropylene fibers (PPF)

As the temperature in the micro-fiber reinforced concrete rises the PP softens and begins to melt due to a progressive change of phase which starts at approximately 150°C when the crystallinity begins to break down into an amorphous polymer. It peaks at 165°C (the commonly quoted melting point), and is complete at approximately 175°C. It is this melting that is believed to facilitate the reduction in the internal stresses in the concrete that cause the explosive spalling. There are two main theories as to how the micro-fibers do this.

A) Mechanisms.

While recognizing the possibility of other mechanisms, [Khoury, 2008], advocates what he terms a PITS (Pressure Induced Tangential Space) theory in which the steam overrides the expansion of the PP as it melts, to squeeze between the micro-fibers and the concrete matrix and pass along the length of the fiber. He claims that the effectiveness of such a mechanism would be dependent upon the cumulative surface area of the micro-fiber and connectivity of the fibers, and is therefore favored by an ultrafine fiber with a diameter of around 18µm that provides a very high number of fibers. Since micro-fibers are dispersed throughout the concrete it is not clear how the connectivity of the fibers is created and how the steam pressure is alleviated. This theory also cannot explain why 32µm diameter micro-fibers - that provide only one third the number of fibers compared to 18µm diameter - have been proven to provide comparable and possibly slightly superior explosive spalling resistance [Jansson et al, 2008].

B) Microcracking mechanism.

An alternative theory presented by Sullivan (2001) contends that as an individual PP fiber melts, its much higher coefficient of thermal expansion compared to that of concrete (8.5x) creates a large number of micro-cracks. These newly created micro-cracks can then link with the micro-cracks created by the thermal expansion of neighboring micro-fibers, or from thermally induced stresses, to form an interconnecting network that can facilitate the movement of steam through the concrete. It is this permeability, which is created, most importantly, only should a fire event occur, that relieves the stresses created by the steam generation and counteracts the possibility of explosive spalling. [Liu et al, 2008] found from backscattering electron microscopy (BSE) and gas permeability testing that the melting of the PP fibers increased the connectivity of the isolated pores leading to an increase in permeability, with peak permeability occurring at approximately 200°C or soon after the melting point of the polypropylene. It was concluded that the creation of micro-cracks and their connectivity into a network as seen in **Fig 2.51** are major factors in determining the permeability of concrete upon exposure to high temperatures.



Fig 2.51-Microcracking network

From preliminary numerical simulation studies, [Saka et al ,2009] reports that a single PP fiber embedded in a mortar matrix and subjected to a temperature increase of 140°C creates a significant stress on the matrix because of the difference in the coefficients of thermal expansion. [Khoury,2008] also indicates a significant tensile stress is exerted on the surrounding matrix by the large difference in thermal expansion between concrete and PP polymer leading to the creation of micro-cracks. Micro-cracks are also created in concrete by thermal effects such as aggregate expansion, drying shrinkage and steam generation. However, it is the supplementary creation of micro-cracks provided by the melting of the PP micro-fibers that operates in a serial/parallel system with these pores and interfacial transition zones [Kalifa et al, 2001] that provides the superior level of protection of the concrete against explosive spalling. The larger the mass of the individual fiber, the higher will be the stress that the molten polymer can create and the increased tendency for micro-cracks to be formed as a result of this stress. Too large an individual fiber however, leads to a lower number of fibers distributed throughout the concrete which reduces the network formation possibilities. Equally, at the other extreme, too small an individual fiber reduces the tendency for micro-cracks to be formed, restricting the network that can be created, which reduces the overall ability of the fiber to prevent explosive spalling [Bostrom and Jansson, 2007]. The optimum size of the fiber for the most efficient explosive spalling resistance lies between these two extremes.

2.16 Scanning electron microscope.

The scanning electron microscope (SEM) is a powerful tool for imaging and chemical analysis in cement research. With a high resolution (down to 1nm) and a large depth of focus, it enables a detailed study of the rough surfaces of e.g. the formed calcium silicate hydrate (C-S-H). This is difficult to study using an optical microscope. The SEM is a microscope that uses electrons instead of light to form an image and it is used under vacuum conditions. A beam of electrons is generated by placing a high electric potential difference between a tip and a plate with an aperture. The potential can range from a few hundred volts to several tens of kilovolts. The electron beam travels through the microscope, where a series of magnetic lenses and apertures focus the electron beam. As the electron beam hits the sample, it will scan the surface in a raster scan pattern, hence the name of the technique. When the focused electron beam hits the sample, the beam electrons will interact with the atoms at or near the surface of the sample and a variety of signals is generated. There are mainly three signals measured in the SEM: secondary (SE) and backscattered (BSE) electrons (for imaging) and characteristic X-rays (for chemical analysis). They originate from different depths and volumes in the sample and provide different information about the sample. The SEM images in this work are all taken in secondary electron detection mode. Using secondary electrons for imaging will show morphology and surface topography of a sample. The secondary electrons originate from the outermost part of the surface and are generated when the beam electrons lose energy by inelastic collisions in the sample and knock out secondary electrons from the atoms. It is primarily the incident beam electrons that knock out the secondary electrons, although backscattered electrons can also contribute.

The energy of secondary electrons is typically 50 eV or less. It is only the secondary electrons generated close to the sample surface that will have sufficient energy to leave the sample. The emitted secondary electrons are attracted to the detector by a positive electric potential and induce a signal. This results in a topological view of the surface that resembles a normal photograph.

2.17 Repair techniques.

Any concrete exposed to temperature more than 300° C should be removed and replaced. Below this temperature, concrete can be repaired by increasing the overall dimensions to take the design load. Based on the results of a thorough and well-planned damage assessment of a fire-damaged concrete structure, an appropriate repair technique can be selected from a range of

techniques including manually applied patching, pneumatically-applied patching, and composite strengthening. In cases where a fire has caused severe distortion to the structure and produced distress in both the concrete and the reinforcing steel, demolition and reconstruction may be required.

2.17.1 Manually applied patching.

Manually applied patching is the simplest, but is typically limited to small areas of repair where localized spall damage has occurred. Repair products include polymer and silica fume modified cementitious mortars and epoxies. These products typically provide high compressive strength and early strength gain for a fast repair cycle and are formulated for horizontal, vertical, and overhead applications. This type of application typically does not generate much noise and can be performed during normal business hours; however, surface preparation operations can be loud and will often have to be limited to off-peak hours if the structure remains occupied.

2.17.2 Pneumatically applied patching

When larger spalled areas must be repaired, pneumatic application of repair mortar (shotcreting) may be more cost effective because larger areas can be covered in less time than with manual applications. This process is loud and messy, and the repair is preferably performed when the building is not occupied.

2.17.3 Composite strengthening

When time is a critical factor or when space is limited, composite materials such as carbon fiber-reinforced polymer (CFRP) or glass fiber-reinforced polymer (GFRP) may be justified repair options. The composite materials typically come in pliable sheets that can conform to their substrate. They are also available in prefabricated solid strips that typically attach to the bottom of beams and slabs depending on the type of repair necessary and the structural element to be repaired. Because epoxies are used to provide adhesion to the substrate of these composite materials, additional fireproofing materials must be installed to protect the repair materials. This repair approach doesn't generate much noise after the surface has been prepared. In spite of the cost, this option becomes viable when the facility must remain open 24 hours a day and when noise is an issue.